Chapter 9

Stimulated Brillouin and Stimulated Rayleigh Scattering

9.1 Stimulated Scattering Processes

We saw in Section 8.1 that light scattering can occur only as the result of fluctuations in the optical properties of a material system. A light-scattering process is said to be *spontaneous* if the fluctuations (typically in the dielectric constant) that cause the light-scattering are excited by thermal or by quantum-mechanical zero-point effects. In contrast, a light-scattering process is said to be *stimulated* if the fluctuations are induced by the presence of the light field. Stimulated light scattering is typically very much more efficient than spontaneous light scattering. For example, approximately one part in 10^5 of the power contained in a beam of visible light would be scattered out of the beam by spontaneous scattering in passing through 1 cm of liquid water.* In this chapter, we shall see that when the intensity of the incident light is sufficiently large, essentially 100% of a beam of light can be scattered in a 1-cm path as the result of stimulated scattering processes.

In the present chapter we study stimulated light scattering resulting from induced density variations of a material system. The most important example of such a process is stimulated Brillouin scattering (SBS), which is illustrated schematically in Fig. 9.1.1. This figure shows an incident laser beam of frequency ω_L scattering from the refractive index variation associated with a sound wave of frequency Ω. Since the acoustic wavefronts are moving away from the incident laser wave, the scattered light is shifted downward in frequency to the Stokes frequency $\omega_S = \omega_L - \Omega$. The reason why this interaction can lead to stimulated light scattering is that the interference of the laser and Stokes fields contains a frequency component at the difference frequency $\omega_L - \omega_S$, which of course is just equal to the frequency Ω of the sound wave. The response of the material system to this interference term can act as a source that tends to increase the amplitude of the sound wave. Thus the beating of the laser wave with the sound wave tends

* Recall that the scattering coefficient R is of the order of 10^{-6} cm^{-1} for water.

Nonlinear Optics. https://doi.org/10.1016/B978-0-12-811002-7.00018-7

to reinforce the Stokes wave, whereas the beating of the laser wave and Stokes waves tends to reinforce the sound wave. Under proper circumstances, the positive feedback described by these two interactions leads to exponential growth of the amplitude of the Stokes wave. SBS was first observed experimentally by Chiao et al. (1964).

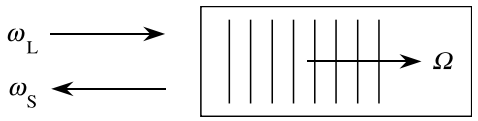

FIGURE 9.1.1: Stimulated Brillouin scattering. Laser light of frequency ω_L scatters from a retreating sound wave of frequency Ω to generate light at the Stokes frequency $\omega_S = \omega_L - \Omega$.

There are two different physical mechanisms by which the interference of the laser and Stokes waves can drive the acoustic wave. One mechanism is electrostriction—that is, the tendency of materials to become more dense in regions of high optical intensity; this process is described in detail in the next section. The other mechanism is optical absorption. The heat evolved by absorption in regions of high optical intensity tends to cause the material to expand in those regions. The density variation induced by this effect can excite an acoustic disturbance. Absorptive SBS is less commonly used than electrostrictive SBS, since it can occur only in lossy optical media. For this reason we shall treat the electrostrictive case first and return to the case of absorptive coupling in Section 9.6.

There are two conceptually different configurations in which SBS can be studied. One is the SBS generator shown in part (a) of Fig. 9.1.2. In this configuration only the laser beam is applied externally, and both the Stokes and acoustic fields grow from noise within the interaction region. The noise process that initiates SBS is typically the scattering of laser light from thermally generated phonons. For the generator configuration, the Stokes radiation is created at frequencies near that for which the gain of the SBS process is largest. We shall see in Section 9.3 how to calculate this frequency.

Part (b) of Fig. 9.1.2 shows an SBS amplifier. In this configuration both the laser and Stokes fields are applied externally. Strong coupling occurs in this case only if the frequency of the injected Stokes wave is approximately equal to the frequency that would be created by an SBS generator.

In Figs. 9.1.1 and 9.1.2, we have assumed that the laser and Stokes waves are counterpropagating. In fact, the SBS process leads to amplification of a Stokes wave propagating in any direction except for the propagation direction of the laser wave.* However, SBS is usually observed only in the backward direction, because the spatial overlap of the laser and Stokes beams is largest under these conditions.

* We shall see in Section 9.3 that copropagating laser and Stokes waves could interact only by means of acoustic waves of infinite wavelength, which cannot occur in a medium of finite spatial extent.

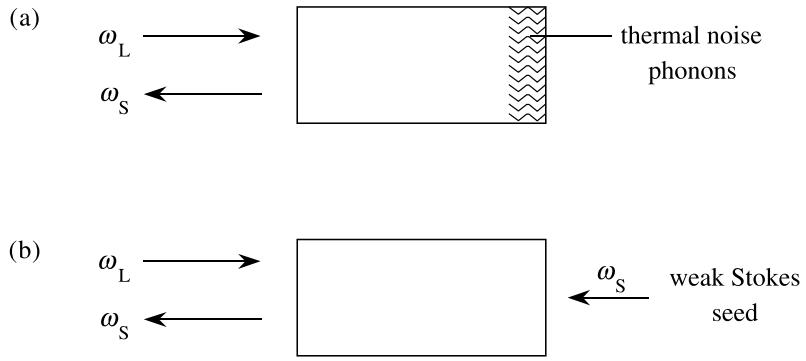

FIGURE 9.1.2: (a) An SBS generator; (b) an SBS amplifier.

9.2 Electrostriction

Electrostriction is the tendency of materials to become compressed in the presence of an electric field. Electrostriction is of interest both as a mechanism leading to a third-order nonlinear optical response and as a coupling mechanism that leads to stimulated Brillouin scattering.

The origin of the effect can be explained in terms of the behavior of a dielectric slab placed in the fringing field of a plane-parallel capacitor. As illustrated in part (a) of Fig. 9.2.1, the slab

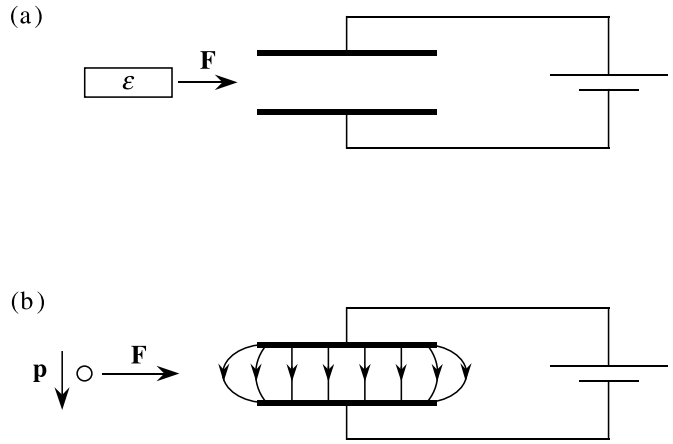

FIGURE 9.2.1: Origin of electrostriction: (a) a dielectric slab placed near a parallel-plate capacitor will be drawn into the region between the capacitor plates. (b) A molecule placed in the fringing field of a parallel-plate capacitor will develop a dipole moment **p** and will thus experience a force in the direction of increasing field strength.

will experience a force tending to pull it into the region of maximum field strength. The nature of this force can be understood either globally or locally.

We can understand the origin of the electrostrictive force from a global point of view as being a consequence of the maximization of stored energy. The potential energy per unit volume of a material located in an electric field of field strength E is changed with respect to its value in the absence of the field by the amount

$$u = \tfrac{1}{2}\epsilon\epsilon_0 E^2, \tag{9.2.1}$$

where ϵ is the relative dielectric constant of the material and ϵ_0 is the permittivity of free space. Consequently the total energy of the system, $\int u\, dV$, is maximized by allowing the slab to move into the region between the capacitor plates where the field strength is largest.

From a microscopic point of view, we can consider the force acting on an individual molecule placed in the fringing field of the capacitor, as shown in part (b) of Fig. 9.2.1. In the presence of the field $\mathbf{E}$, the molecule develops the dipole moment $\mathbf{p} = \epsilon_0\alpha\mathbf{E}$, where α is the molecular polarizability. The energy stored in the polarization of the molecule is given by

$$U = -\int_0^{\mathbf{E}} \mathbf{p}\cdot d\mathbf{E}' = -\int_0^{\mathbf{E}} \epsilon_0\alpha\mathbf{E}'\cdot d\mathbf{E}' = -\tfrac{1}{2}\epsilon_0\alpha\mathbf{E}\cdot\mathbf{E} \equiv -\tfrac{1}{2}\epsilon_0\alpha E^2. \tag{9.2.2}$$

The force acting on the molecule is then given by

$$\mathbf{F} = -\nabla U = \tfrac{1}{2}\epsilon_0\alpha\nabla\left(E^2\right). \tag{9.2.3}$$

We see that each molecule is pulled into the region of increasing field strength.

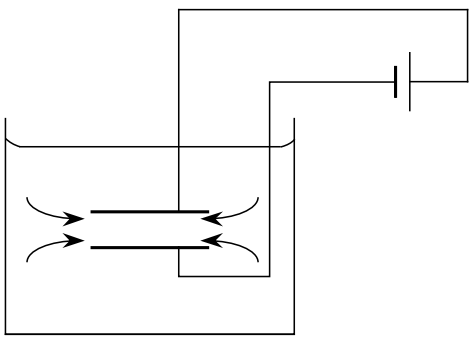

FIGURE 9.2.2: Capacitor immersed in a dielectric liquid.

Next we consider the situation illustrated in Fig. 9.2.2, in which the capacitor is immersed in the dielectric liquid. Molecules are pulled from the surrounding medium into the region between the capacitor plates, thus increasing the density in this region by an amount that we

shall call $\Delta\rho$. We calculate the value of $\Delta\rho$ by means of the following argument: As a result of the increase in density of the material, its dielectric constant changes from its original value ϵ to the value $\epsilon + \Delta\epsilon$, where

$$\Delta\epsilon = \left(\frac{\partial\epsilon}{\partial\rho}\right)\Delta\rho. \tag{9.2.4}$$

Consequently, the field energy density of Eq. (9.2.1) changes by the amount

$$\Delta u = \tfrac{1}{2}\epsilon_0 E^2 \Delta\epsilon = \tfrac{1}{2}\epsilon_0 E^2 \left(\frac{\partial\epsilon}{\partial\rho}\right)\Delta\rho. \tag{9.2.5}$$

However, according to the first law of thermodynamics, this change in energy Δu must be equal to the work performed in compressing the material; the work done per unit volume is given by

$$\Delta w = p_{\text{st}}\frac{\Delta V}{V} = -p_{\text{st}}\frac{\Delta\rho}{\rho}. \tag{9.2.6}$$

Here the strictive pressure p_{st} is the contribution to the pressure of the material that is due to the presence of the electric field. Since $\Delta u = \Delta w$, by equating Eqs. (9.2.5) and (9.2.6), we find that the electrostrictive pressure is given by

$$p_{\text{st}} = -\tfrac{1}{2}\epsilon_0\rho\left(\frac{\partial\epsilon}{\partial\rho}\right)E^2 \equiv -\tfrac{1}{2}\epsilon_0\gamma_e E^2, \tag{9.2.7}$$

where $\gamma_e = \rho(\partial\epsilon/\partial\rho)$ is known as the electrostrictive constant (see also Eq. (8.3.6)). Since p_{st} is negative, the total pressure is reduced in regions of high field strength. The fluid tends to be drawn into these regions, and the density increases. We calculate the change in density as $\Delta\rho = -(\partial\rho/\partial p)\Delta p$, where we equate Δp with the electrostrictive pressure of Eq. (9.2.7). We write this result as

$$\Delta\rho = -\rho\left(\frac{1}{\rho}\frac{\partial\rho}{\partial p}\right)p_{\text{st}} \equiv -\rho C p_{\text{st}}, \tag{9.2.8}$$

where $C = \rho^{-1}(\partial\rho/\partial p)$ is the compressibility. Combining this result with Eq. (9.2.7), we find that

$$\Delta\rho = \tfrac{1}{2}\epsilon_0\rho C\gamma_e E^2. \tag{9.2.9}$$

This equation describes the change in material density $\Delta\rho$ induced by an applied electric field of strength E.

The derivation of this expression for $\Delta\rho$ has implicitly assumed that the electric field E is a static field. In such a case, the derivatives that appear in the expressions for C and γ_e are to be performed with the temperature T held constant. However, our primary interest is for the case

in which E represents an optical frequency field; in such a case Eq. (9.2.9) should be replaced by

$$\Delta\rho = \tfrac{1}{2}\epsilon_0 \rho C \gamma_e \langle \tilde{\mathbf{E}} \cdot \tilde{\mathbf{E}} \rangle, \tag{9.2.10}$$

where the angular brackets denote a time average over an optical period. If $\tilde{\mathbf{E}}(t)$ contains more than one frequency component so that $\langle \tilde{\mathbf{E}} \cdot \tilde{\mathbf{E}} \rangle$ contains both static components and hypersonic components (as in the case of SBS), C and γ_e should be evaluated at constant entropy to determine the response for the hypersonic components and at constant temperature to determine the response for the static components.

Let us consider the modification of the optical properties of a material system that occurs as a result of electrostriction. We represent the change in the susceptibility in the presence of an optical field as $\Delta\chi = \Delta\epsilon$, where $\Delta\epsilon$ is calculated as $(\partial\epsilon/\partial\rho)\Delta\rho$, with $\Delta\rho$ given by Eq. (9.2.10). We thus find that

$$\Delta\chi = \tfrac{1}{2}\epsilon_0 C \gamma_e^2 \langle \tilde{\mathbf{E}} \cdot \tilde{\mathbf{E}} \rangle. \tag{9.2.11}$$

For the present, let us consider the case of a monochromatic applied field

$$\tilde{\mathbf{E}}(t) = \mathbf{E} e^{-i\omega t} + \text{c.c.}; \tag{9.2.12}$$

the case in which $\tilde{\mathbf{E}}(t)$ contains two frequency components that differ by approximately the Brillouin frequency is treated in the following section on SBS. Then, since $\langle \tilde{\mathbf{E}} \cdot \tilde{\mathbf{E}} \rangle = 2\mathbf{E} \cdot \mathbf{E}^*$, we see that

$$\Delta\chi = \epsilon_0 C_T \gamma_e^2 \mathbf{E} \cdot \mathbf{E}^*. \tag{9.2.13}$$

The complex amplitude of the nonlinear polarization that results from this change in the susceptibility can be represented as $\mathbf{P} = \Delta\chi \mathbf{E}$, that is, as

$$\mathbf{P} = \epsilon_0 C_T \gamma_e^2 |\mathbf{E}|^2 \mathbf{E}. \tag{9.2.14}$$

If we write this result in terms of a conventional third-order susceptibility, defined through

$$\mathbf{P} = 3\epsilon_0 \chi^{(3)}(\omega = \omega + \omega - \omega)|\mathbf{E}|^2 \mathbf{E}, \tag{9.2.15}$$

we find that

$$\chi^{(3)}(\omega = \omega + \omega - \omega) = \tfrac{1}{3} C_T \gamma_e^2. \tag{9.2.16}$$

For simplicity, we have suppressed the tensor nature of the nonlinear susceptibility in the foregoing discussion. However, we can see from the form of Eq. (9.2.14) that, for an isotropic material, the nonlinear coefficients of Maker and Terhune (see Eq. (4.2.10)) have the form $A = C_T \gamma_e^2$ and $B = 0$.

Let us estimate the numerical value of $\chi^{(3)}$. We saw in Eq. (8.3.12) that for a dilute gas the electrostrictive constant $\gamma_e \equiv \rho(\partial\epsilon/\partial\rho)$ is given by $\gamma_e = n^2 - 1$. More generally, we can estimate γ_e through use of the Lorentz–Lorenz law (Eq. (3.9.8a)), which leads to the prediction

$$\gamma_e = \left(n^2 - 1\right)\left(n^2 + 2\right)/3. \tag{9.2.17}$$

This result shows that γ_e is of the order of unity for condensed matter. The compressibility $C_T = \rho^{-1}(\partial\rho/\partial p)$ is approximately equal to 10^{-9} $\mathrm{m^2\,Nt^{-1}}$ for CS_2 and is of the same order of magnitude for all condensed matter. We thus find that $\chi^{(3)}(\omega = \omega + \omega - \omega)$ is of the order of 3×10^{-21} $\mathrm{m^2\ V^{-2}}$ for condensed matter. For ideal gases, the compressibility C_T is equal to $1/p$, where at 1 atmosphere $p = 10^5$ $\mathrm{Nt/m^2}$. The electrostrictive constant $\gamma_e = n^2 - 1$ for air at 1 atmosphere is approximately equal to 6×10^{-4}. We thus find that $\chi^{(3)}(\omega = \omega + \omega - \omega)$ is of the order of 1×10^{-23} $\mathrm{m^2\,V^{-2}}$ for gases at 1 atmosphere of pressure.

A very useful, alternative expression for $\chi^{(3)}(\omega = \omega + \omega - \omega)$ can be deduced from expression (9.2.16) by expressing the electrostrictive constant in terms of the refractive index through use of Eq. (9.2.17) and by expressing the compressibility in terms of the material density and velocity of sound through use of Eq. (8.3.21), such that $C_s = 1/v^2\rho$. Similarly, the isothermal compressibility is given by $C_T = \gamma C_s$ where γ is the usual thermodynamic adiabatic index. One thus finds that

$$\chi^{(3)}(\omega = \omega + \omega - \omega) = \frac{\epsilon_0 \gamma}{3v^2\rho}\left[\frac{(n^2 - 1)(n^2 + 2)}{3}\right]^2. \tag{9.2.18}$$

For pulses sufficiently short that heat flow during the pulse is negligible, the factor of γ in the numerator of this expression is to be replaced by unity. As usual, the nonlinear refractive index coefficient n_2 for electrostriction can be deduced from this expression and the result $n_2 = (3/4n_0^2\epsilon_0 c)\chi^{(3)}$ obtained earlier (Eq. (4.1.19)).

In comparison with other types of optical nonlinearities, the value of $\chi^{(3)}$ resulting from electrostriction is not usually large. However, it can make an appreciable contribution to total measured nonlinearity for certain optical materials. For the case of optical fibers, Buckland and Boyd (1996, 1997) found that electrostriction can make an approximately 20% contribution to the third-order susceptibility. Moreover, we shall see in the next section that electrostriction provides the nonlinear coupling that leads to stimulated Brillouin scattering, which is often an extremely strong process.

9.3 Stimulated Brillouin Scattering (Induced by Electrostriction)

Our discussion of spontaneous Brillouin scattering in Chapter 8 presupposed that the applied optical fields are sufficiently weak that they do not alter the acoustic properties of the material system. Spontaneous Brillouin scattering then results from the scattering of the incident radiation off the sound waves that are thermally excited.

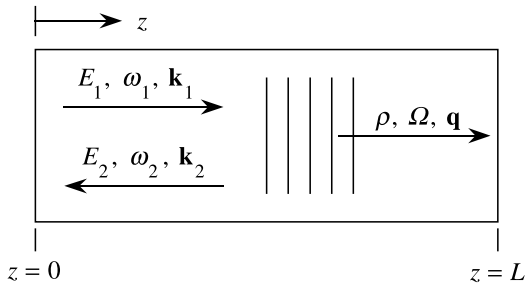

FIGURE 9.3.1: Schematic representation of the stimulated Brillouin scattering process.

For an incident laser field of sufficient intensity, even the spontaneously scattered light can become quite intense. This scattered light field can then beat with the incident laser beam, and through the process of electrostriction* can thereby induce density variations. The incident laser field can then scatter off the refractive index variation that accompanies these density variations. The scattered light will be at the Stokes frequency and will add constructively with the Stokes radiation that produced the acoustic disturbance. In this manner, the acoustic and Stokes waves mutually reinforce each other's growth, and each can grow to a large amplitude. This circumstance is depicted in Fig. 9.3.1. Here an incident wave of amplitude E_1, angular frequency ω_1, and wavevector $\mathbf{k}_1$ scatters off a retreating sound wave of amplitude ρ, frequency Ω, and wavevector $\mathbf{q}$ to form a scattered wave of amplitude E_2, frequency ω_2, and wavevector $\mathbf{k}_2$.†

Let us next deduce the frequency ω_2 of the Stokes field that is created by the SBS process for the case of an SBS generator (see also part (a) of Fig. 9.1.2). Since the laser field at frequency ω_1 is scattered from a retreating sound wave, the scattered radiation will be shifted downward in frequency to

$$\omega_2 = \omega_1 - \Omega_B. \tag{9.3.1}$$

Here Ω_B is called the Brillouin frequency, and we shall now see how to determine its value. The Brillouin frequency is related to the acoustic wavevector $\mathbf{q}_B$ by the phonon dispersion relation

$$\Omega_B = |\mathbf{q}_B| v, \tag{9.3.2}$$

where v is the velocity of sound. By assumption, this sound wave is driven by the beating of the laser and Stokes fields, and its wavevector is therefore given by

$$\mathbf{q}_B = \mathbf{k}_1 - \mathbf{k}_2. \tag{9.3.3}$$

* Stimulated Brillouin scattering can also be induced by absorptive effects. This less commonly studied case is examined in Section 9.6.

† We denote the field frequencies as ω_1 and ω_2 rather than ω_L and ω_S so that we can apply the results of the present treatment to the case of anti-Stokes scattering by identifying ω_1 with ω_{aS} and ω_2 with ω_L. The treatment of the present section assumes only that $\omega_2 < \omega_1$.

Since the wavevectors and frequencies of the optical waves are related in the usual manner, that is, by $|\mathbf{k}_i| = n\omega_i/c$, we can use Eq. (9.3.3) and the fact that the laser and Stokes waves are counterpropagating to express the Brillouin frequency of Eq. (9.3.2) as

$$\Omega_B = \frac{v}{c/n}(\omega_1 + \omega_2). \tag{9.3.4}$$

Eqs. (9.3.1) and (9.3.4) are now solved simultaneously to obtain an expression for the Brillouin frequency in terms of the frequency ω_1 of the applied field only—that is, we eliminate ω_2 from these equations to obtain

$$\Omega_B = \frac{\dfrac{2v}{c/n}\omega_1}{1 + \dfrac{v}{c/n}}. \tag{9.3.5}$$

However, since v is very much smaller than c/n for all known materials, it is an excellent approximation to take the Brillouin frequency to be simply

$$\Omega_B = \frac{2v}{c/n}\omega_1. \tag{9.3.6}$$

At this same level of approximation, the acoustic wavevector is given by

$$\mathbf{q}_B = 2\mathbf{k}_1. \tag{9.3.7}$$

For the case of the SBS amplifier configuration (see part (b) of Fig. 9.1.2), the Stokes wave is imposed externally and its frequency ω_2 is known *a priori*. The frequency of the driven acoustic wave is then given by

$$\Omega = \omega_1 - \omega_2, \tag{9.3.8}$$

which in general will be different from the Brillouin frequency of Eq. (9.3.6). As we shall see below, the acoustic wave will be excited efficiently under these circumstances only when ω_2 is chosen such that the frequency difference $|\Omega - \Omega_B|$ is less than or of the order of the Brillouin linewidth Γ_B, which is defined in Eq. (9.3.14b).

Let us next see how to treat the nonlinear coupling among the three interacting waves. We represent the optical field within the Brillouin medium as $\tilde{E}(z,t) = \tilde{E}_1(z,t) + \tilde{E}_2(z,t)$, where

$$\tilde{E}_1(z,t) = A_1(z,t)e^{i(k_1 z - \omega_1 t)} + \text{c.c.} \tag{9.3.9a}$$

and

$$\tilde{E}_2(z,t) = A_2(z,t)e^{i(-k_2 z - \omega_2 t)} + \text{c.c.} \tag{9.3.9b}$$

Similarly, we describe the acoustic field in terms of the material density distribution

$$\tilde{\rho}(z,t) = \rho_0 + \left[\rho(z,t)e^{i(qz-\Omega t)} + \text{c.c.}\right], \tag{9.3.10}$$

where $\Omega = \omega_1 - \omega_2$, $q = 2k_1$, and ρ_0 denotes the mean density of the medium.

We assume that the material density obeys the acoustic wave equation (see also Eq. (8.3.17))

$$\frac{\partial^2\tilde{\rho}}{\partial t^2} - \Gamma'\nabla^2\frac{\partial\tilde{\rho}}{\partial t} - v^2\nabla^2\tilde{\rho} = \nabla\cdot\mathbf{f}, \tag{9.3.11}$$

where v is the velocity of sound and Γ' is a damping parameter given by Eq. (8.3.23). The source term on the right-hand side of this equation consists of the divergence of the force per unit volume $\mathbf{f}$, which is given explicitly by

$$\mathbf{f} = \nabla p_{\text{st}}, \quad p_{\text{st}} = -\tfrac{1}{2}\epsilon_0\gamma_e\langle\tilde{E}^2\rangle. \tag{9.3.12}$$

For the fields given by Eq. (9.3.9), this source term is given by

$$\nabla\cdot\mathbf{f} = \epsilon_0\gamma_e q^2\left[A_1A_2^*e^{i(qz-\Omega t)} + \text{c.c.}\right]. \tag{9.3.13}$$

If we now introduce Eqs. (9.3.10) and (9.3.13) into the acoustic wave equation (9.3.11) and assume that the acoustic amplitude varies slowly (if at all) in space and time, we obtain the result

$$-2i\Omega\frac{\partial\rho}{\partial t} + \left(\Omega_{\text{B}}^2 - \Omega^2 - i\Omega\Gamma_{\text{B}}\right)\rho - 2iqv^2\frac{\partial\rho}{\partial z} = \epsilon_0\gamma_e q^2A_1A_2^*, \tag{9.3.14a}$$

where we have introduced the Brillouin linewidth

$$\Gamma_{\text{B}} = q^2\Gamma'; \tag{9.3.14b}$$

its reciprocal $\tau_p = \Gamma_{\text{B}}^{-1}$ gives the phonon lifetime.

Eq. (9.3.14a) can often be simplified substantially by omitting the last term on its left-hand side. This term describes the propagation of phonons. However, hypersonic phonons are strongly damped and thus propagate only over very short distances before being absorbed.* Since the phonon propagation distance is typically small compared to the distance over which the source term on the right-hand side of Eq. (9.3.14a) varies significantly, it is conventional to drop the term containing $\partial\rho/\partial z$ in describing SBS. This approximation can break down, however, as discussed by Chiao (1965) and by Kroll and Kelley (1971). If we drop the spatial

* We can estimate this distance as follows: According to Eq. (8.3.30), the sound absorption coefficient is given by $\alpha_s = \Gamma_{\text{B}}/v$, whereby in Eqs. (8.3.23) and (8.3.28) Γ_{B} is of the order of $\eta_s q^2/\rho_0$. For the typical values $v = 1\times10^3$ m/sec, $\eta_s = 10^{-9}$ N m/sec^2, $q = 4\pi\times10^6$ m^{-1}, and $\rho_0 = 10$ kg m^{-3}, we find that $\Gamma_{\text{B}} = 1.6\times10^8$ sec^{-1} and $\alpha_s^{-1} = 6.3$ μm.

derivative term in Eq. (9.3.14a) and assume steady-state conditions so that $\partial\rho/\partial t$ also vanishes, we find that the acoustic amplitude is given by

$$\rho(z,t) = \epsilon_0 \gamma_e q^2 \frac{A_1 A_2^*}{\Omega_B^2 - \Omega^2 - i\Omega\Gamma_B}. \tag{9.3.15}$$

We turn now to the description of the spatial evolution of the optical fields, which is described by the wave equation

$$\frac{\partial^2 \tilde{E}_i}{\partial z^2} - \frac{1}{(c/n)^2}\frac{\partial^2 \tilde{E}_i}{\partial t^2} = \frac{1}{\epsilon_0 c^2}\frac{\partial^2 \tilde{P}_i}{\partial t^2}, \quad i = 1, 2. \tag{9.3.16}$$

The total nonlinear polarization, which gives rise to the source term in this equation, is given by

$$\tilde{P} = \epsilon_0 \Delta\chi \tilde{E} = \epsilon_0 \Delta\epsilon \tilde{E} = \epsilon_0 \rho_0^{-1} \gamma_e \tilde{\rho} \tilde{E}. \tag{9.3.17}$$

We next determine those parts of $\tilde{P}$ that can act as phase-matched source terms for the laser and Stokes fields. These contributions are given by

$$\tilde{P}_1 = p_1 e^{i(k_1 z - \omega_1 t)} + \text{c.c.}, \qquad \tilde{P}_2 = p_2 e^{i(-k_2 z - \omega_2 t)} + \text{c.c.}, \tag{9.3.18}$$

where

$$p_1 = \epsilon_0 \gamma_e \rho_0^{-1} \rho A_2, \qquad p_2 = \epsilon_0 \gamma_e \rho_0^{-1} \rho^* A_1. \tag{9.3.19}$$

We introduce Eqs. (9.3.9) into the wave equation (9.3.16) along with Eqs. (9.3.18) and (9.3.19), make the slowly-varying amplitude approximation, and obtain the equations

$$\frac{\partial A_1}{\partial z} + \frac{1}{c/n}\frac{\partial A_1}{\partial t} = \frac{i\omega\gamma_e}{2nc\rho_0}\rho A_2, \tag{9.3.20a}$$

$$-\frac{\partial A_2}{\partial z} + \frac{1}{c/n}\frac{\partial A_2}{\partial t} = \frac{i\omega\gamma_e}{2nc\rho_0}\rho^* A_1. \tag{9.3.20b}$$

In these equations ρ is given by the solution to Eq. (9.3.14a). Furthermore, we have dropped the distinction between ω_1 and ω_2 by setting $\omega = \omega_1 \simeq \omega_2$.

Let us now consider steady-state conditions. In this case the time derivatives appearing in Eqs. (9.3.20) can be dropped, and ρ is given by Eq. (9.3.15). The coupled-amplitude equations then become

$$\frac{dA_1}{dz} = \frac{i\epsilon_0\omega q^2\gamma_e^2}{2nc\rho_0}\frac{|A_2|^2 A_1}{\Omega_B^2 - \Omega^2 - i\Omega\Gamma_B}, \tag{9.3.21a}$$

$$\frac{dA_2}{dz} = \frac{-i\epsilon_0\omega q^2\gamma_e^2}{2nc\rho_0}\frac{|A_1|^2 A_2}{\Omega_B^2 - \Omega^2 + i\Omega\Gamma_B}. \tag{9.3.21b}$$

We see from the form of these equations that SBS is a pure gain process, that is, that the SBS process is automatically phase-matched. For this reason, it is possible to introduce coupled equations for the intensities of the two interacting optical waves. Defining the intensities as $I_i = 2n\epsilon_0 c A_i A_i^*$, we find from Eqs. (9.3.21) that

$$\frac{dI_1}{dz} = -gI_1I_2 \tag{9.3.22a}$$

and

$$\frac{dI_2}{dz} = -gI_1I_2. \tag{9.3.22b}$$

In these equations g is the SBS gain factor, which to good approximation is given by

$$g = g_0 \frac{(\Gamma_B/2)^2}{(\Omega_B - \Omega)^2 + (\Gamma_B/2)^2}, \tag{9.3.23}$$

where the line-center gain factor is given by

$$g_0 = \frac{\gamma_e^2 \omega^2}{nvc^3 \rho_0 \Gamma_B}. \tag{9.3.24}$$

The solution to Eqs. (9.3.22) under general conditions is described below. Note, however, that in the constant-pump limit $I_1 =$ constant, the solution to Eq. (9.3.22b) is

$$I_2(z) = I_2(L)e^{gI_1(L-z)}. \tag{9.3.25}$$

In this limit a Stokes wave injected into the medium at $z = L$ experiences exponential growth as it propagates through the medium. It should be noted that the line-center gain factor g_0 of Eq. (9.3.24) is independent of the laser frequency ω, because the Brillouin linewidth Γ_B is proportional to ω^2 (recall that, according to Eq. (8.3.28), Γ_B is proportional to q^2 and that q is proportional to ω). An estimate of the size of g_0 for the case of CS_2 at a wavelength of 1 μm can be made as follows: $\omega = 2\pi \times 3 \times 10^{14}$ rad/sec, $n = 1.67$, $v = 1.1 \times 10^3$ m/sec, $\rho_0 = 1.26$ g/cm^3 $= 1.26 \times 10^3$ kg/m^3, $\gamma_e = 2.4$, and $\tau_p = \Gamma_B^{-1} = 4 \times 10^{-9}$ sec, giving $g_0 = 1.5$ m/GW, which in conventional laboratory units becomes $g_0 = 0.15$ cm/MW. The Brillouin gain factors and spontaneous linewidths $\Delta\nu = \Gamma_B/2\pi$ are listed in Table 9.3.1 for a variety of materials.

The theoretical treatment just presented can also be used to describe the propagation of a wave at the anti-Stokes frequency, $\omega_{aS} = \omega_L + \Omega_B$. Eqs. (9.3.22) were derived for the geometry of Fig. 9.3.1 under the assumption that $\omega_1 > \omega_2$. We can treat anti-Stokes scattering by identifying ω_1 with ω_{aS} and ω_2 with ω_L. We then find that the constant-pump approximation corresponds to the case $I_2(z) =$ constant and that the solution to Eq. (9.3.22a) is $I_1(z) = I_1(0)e^{-gI_2z}$. Since the anti-Stokes wave at frequency ω_1 propagates in the positive z direction, we see that it experiences attenuation due to the SBS process.

TABLE 9.3.1: Properties of stimulated Brillouin scattering for a variety of materials[a].

Substance	$\Omega_B/2\pi$ (MHz)	$\Gamma_B/2\pi$ (MHz)	g_0 (m/GW)	$g_B^a(\max)/\alpha$ (cm^2/MW)
CS_2	5850	52.3	1.5	0.14
Acetone	4600	224	0.2	0.022
Toluene	5910	579	0.13	
CCl_4	4390	520	0.06	0.013
Methanol	4250	250	0.13	0.013
Ethanol	4550	353	0.12	0.010
Benzene	6470	289	0.18	0.024
H_2O	5690	317	0.048	0.0008
Cyclohexane	5550	774	0.068	
CH_4(1400 atm)	150	10	1	
Optical glasses	15,000–26,000	10–106	0.04–0.25	
SiO_2	25,800	78	0.045	

[a] Values are quoted for a wavelength of 0.694 μm. The quantity $\Gamma_B/2\pi$ is the full width at half maximum in ordinary frequency units of the SBS gain spectrum. The last column gives a parameter used to describe the process of absorptive SBS, which is discussed in Section 9.6. To convert to other laser frequencies ω, recall that Ω_B is proportional to ω, Γ is proportional to ω^2, g_0 is independent of ω, and $g_B^a(\max)$ is proportional to ω^{-3}.

9.3.1 Pump Depletion Effects in SBS

We have seen (Eq. (9.3.25)) that, in the approximation in which the pump intensity is taken to be spatially invariant, the Stokes wave experiences exponential growth as it propagates through the Brillouin medium. Once the Stokes wave has grown to an intensity comparable to that of the pump wave, significant depletion of the pump wave must occur, and under these conditions we must solve the coupled-intensity equations (9.3.22) simultaneously in order to describe the SBS process. To find this simultaneous solution, we first note that $dI_1/dz = dI_2/dz$ and thus that

$$I_1(z) = I_2(z) + C, \tag{9.3.26}$$

where the value of the integration constant C depends on the boundary conditions. Using this result, Eq. (9.3.22b) can be expressed as

$$\frac{dI_2}{I_2(I_2 + C)} = -g\,dz. \tag{9.3.27}$$

This equation can be integrated formally as

$$\int_{I_2(0)}^{I_2(z)} \frac{dI_2}{I_2(I_2 + C)} = -\int_0^z g\,dz', \tag{9.3.28}$$

which implies that

$$\ln\left\{\frac{I_2(z)[I_2(0)+C]}{I_2(0)[I_2(z)+C]}\right\} = -gCz. \tag{9.3.29}$$

Since we have specified the value of I_1 at $z = 0$, it is convenient to express the constant C defined by Eq. (9.3.26) as $C = I_1(0) - I_2(0)$. Eq. (9.3.29) is now solved algebraically for $I_2(z)$, yielding

$$I_2(z) = \frac{I_2(0)[I_1(0) - I_2(0)]}{I_1(0)\exp\{gz[I_1(0) - I_2(0)]\} - I_2(0)}. \tag{9.3.30a}$$

According to Eq. (9.3.26), $I_1(z)$ can be found in terms of this expression as

$$I_1(z) = I_2(z) + I_1(0) - I_2(0). \tag{9.3.30b}$$

Eqs. (9.3.30) give the spatial distribution of the field intensities in terms of the boundary values $I_1(0)$ and $I_2(0)$. However, the boundary values that are known physically are $I_1(0)$ and $I_2(L)$; see Fig. 9.3.2. In order to find the unknown quantity $I_2(0)$ in terms of the known quantities $I_1(0)$ and $I_2(L)$, we set z equal to L in Eq. (9.3.30a) and write the resulting expression as follows:

$$I_2(L) = \frac{I_1(0)[I_2(0)/I_1(0)][1 - I_2(0)/I_1(0)]}{\exp\{gI_1(0)L[1 - I_2(0)/I_1(0)]\} - I_2(0)/I_1(0)}. \tag{9.3.31}$$

This expression is a transcendental equation giving the unknown quantity $I_2(0)/I_1(0)$ in terms of the known quantities $I_1(0)$ and $I_2(L)$.

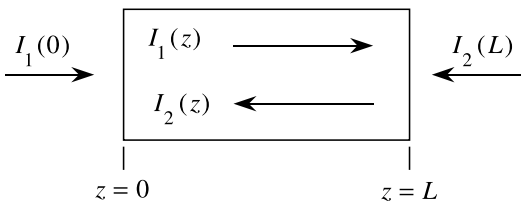

FIGURE 9.3.2: Geometry of an SBS amplifier. The boundary values $I_1(0)$ and $I_2(L)$ are known.

The results given by Eqs. (9.3.30) and (9.3.31) can be used to analyze the SBS amplifier shown in Fig. 9.3.2. The transfer characteristics of such an amplifier are illustrated in Fig. 9.3.3. Here the vertical axis gives the fraction of the laser intensity that is transferred to the Stokes wave, and the horizontal axis is the quantity $G = gI_1(0)L$, which gives the exponential gain experienced by a *weak* Stokes input. The various curves are labeled according to the ratio of input intensities, $I_2(L)/I_1(0)$. For sufficiently large values of the exponential gain, essentially complete transfer of the pump energy to the Stokes beam is possible.

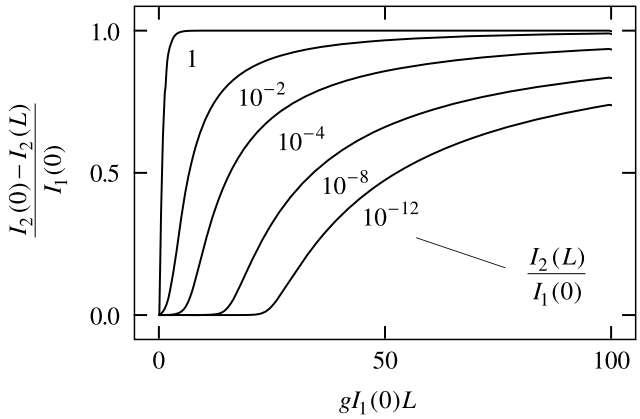

FIGURE 9.3.3: Intensity transfer characteristics of an SBS amplifier.

9.3.2 SBS Generator

For the case of an SBS generator, no Stokes field is injected externally into the interaction region, and thus the value of the Stokes intensity near the Stokes input face $z = L$ is not known *a priori*. In this case, the SBS process is initiated by Stokes photons that are created by spontaneous Brillouin scattering involving the laser beam near its exit plane $z = L$. We therefore expect that the effective Stokes input intensity $I_2(L)$ will be proportional to the local value of the laser intensity $I_1(L)$; we designate the constant of proportionality as f so that

$$I_2(L) = f I_1(L). \tag{9.3.32}$$

We estimate the value of f as follows: We first consider the conditions that apply below the threshold for the occurrence of SBS, that is, under conditions such that the SBS reflectivity $R = I_2(0)/I_1(0)$ is much smaller than unity. Under these conditions the laser intensity is essentially constant throughout the medium, and the Stokes output intensity is related to the Stokes input intensity by $I_2(0) = I_2(L)e^G$, where $G = gI_1(0)L$. However, since $I_2(L) = fI_1(0)$ (because $I_1(z)$ is constant), the SBS reflectivity can be expressed as

$$R \equiv \frac{I_2(0)}{I_1(0)} = fe^G. \tag{9.3.33}$$

Laboratory experience has shown that the SBS process displays an apparent threshold. One often defines the SBS threshold as the condition that the reflectivity R reach some prescribed value R_{th}; the value $R_{\text{th}} = 0.01$ is a convenient choice. This reflectivity occurs for the specific value G_{th} of the gain parameter $G = gI_1(0)L$. For a wide variety of materials and laser wavelengths, it is found that G_{th} typically lies in the fairly narrow range of 25 to 30. The actual value

of G_{th} for a particular situation can be deduced theoretically from a consideration of the thermal fluctuations that initiate the SBS process; see, for instance, Boyd et al. (1990) for details. Since G_{th} is approximately 25–30, we see from Eq. (9.3.33) that f is of the order of $\exp(-G_{\text{th}})$, or approximately 10^{-12} to 10^{-11}. An order-of-magnitude estimate based on the properties of spontaneous scattering performed by Zel'dovich et al. (1985) reaches the same conclusion.

We next calculate the SBS reflectivity R for the general case $G > G_{\text{th}}$ (i.e., above threshold) through use of Eq. (9.3.31), which we write as

$$\frac{I_2(L)}{I_1(0)} = \frac{R(1-R)}{\exp[G(1-R)] - R}. \tag{9.3.34}$$

To good approximation, $-R$ can be dropped from the denominator of the right-hand side of this equation. In order to determine the ratio $I_2(L)/I_1(0)$ that appears on the left-hand side of Eq. (9.3.34), we express Eq. (9.3.30b) as

$$I_1(L) - I_2(L) = I_1(0) - I_2(0).$$

Through use of Eq. (9.3.32) and the smallness of f, we can replace the left-hand side of this equation by $f^{-1}I_2(L)$. We now multiply both sides of the resulting equation by $f/I_1(0)$ to obtain the result $I_2(L)/I_1(0) = f(1-R)$. This expression is substituted for the left-hand side of Eq. (9.3.34), which is then solved for G, yielding the result

$$\frac{G}{G_{\text{th}}} = \frac{G_{\text{th}}^{-1} \ln R + 1}{1-R}, \tag{9.3.35}$$

where we have substituted G_{th} for $-\ln f$.

The nature of this solution is illustrated in Fig. 9.3.4, where the SBS reflectivity $R = I_2(0)/I_1(0)$ is shown plotted as a function of $G = gI_1(0)L$ for the value $G_{\text{th}} = 25$. We see that essentially no Stokes light is created for G less than G_{th} and that the reflectivity rises rapidly for laser intensities slightly above this threshold value. In addition, for $G \gg G_{\text{th}}$ the reflectivity asymptotically approaches 100%. Well above the threshold for SBS (i.e., for $G \gtrsim 3G_{\text{th}}$), Eq. (9.3.35) can be approximated as $G/G_{\text{th}} \simeq 1/(1-R)$, which shows that the SBS reflectivity in this limit can be expressed as

$$R = 1 - \frac{1}{G/G_{\text{th}}} \quad (\text{for} \quad G \gg G_{\text{th}}). \tag{9.3.36}$$

Since the intensity $I_1(L)$ of the transmitted laser beam is given by $I_1(L) = I_1(0)(1-R)$, in the limit of validity of Eq. (9.3.36) the intensity of the transmitted beam is given by

$$I_1(L) = \frac{G_{\text{th}}}{gL}; \tag{9.3.37}$$

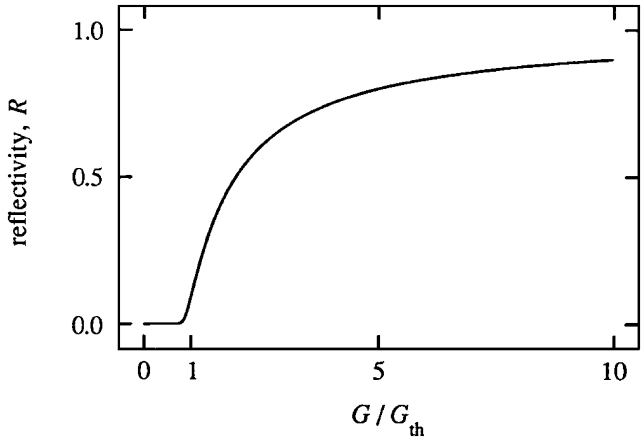

FIGURE 9.3.4: Dependence of the SBS reflectivity on the weak-signal gain $G = gI_1(0)L$.

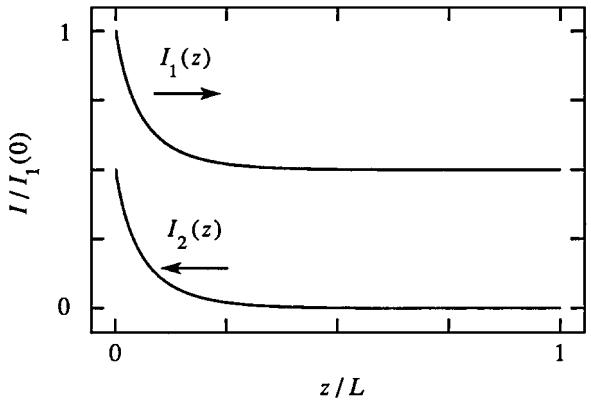

FIGURE 9.3.5: Distribution of the laser and Stokes intensities within the interaction region of an SBS generator.

here G_{th}/gL can be interpreted as the input laser intensity at the threshold for SBS. Hence the transmitted intensity is "clamped" at the threshold value for the occurrence of SBS.

Once the value of the Stokes intensity at the plane $z = 0$ is known from Eq. (9.3.35), the distributions of the intensities within the interaction region can be obtained from Eqs. (9.3.20). Fig. 9.3.5 shows the distribution of intensities within an SBS generator.*

Let us estimate the minimum laser power P_{th} required to excite SBS under optimum conditions. We assume that a laser beam having a gaussian transverse profile is focused tightly

* Fig. 9.3.5 is plotted for the case $G_{\text{th}} = 10$. The physically realistic case of $G_{\text{th}} = 25$ produces a much less interesting graph because the perceptible variation in intensities occurs in a small region near $z = 0$.

into a cell containing a Brillouin-active medium. The characteristic intensity of such a beam at the beam waist is given by $I = P/\pi w_0^2$, where w_0 is the beam waist radius. The interaction length L is limited to the characteristic diffraction length $b = 2\pi w_0^2/\lambda$ of the beam. The product $G = gIL$ is thus given by $G = 2gP/\lambda$, and by equating this expression with the threshold value G_{th} we find that the minimum laser power required to excite SBS is of the order of

$$P_{\text{th}} = \frac{G_{\text{th}}\lambda}{2g}. \tag{9.3.38}$$

For $\lambda = 1.06$ μm, $G_{\text{th}} = 25$, and $g = 0.15$ cm/MW (the value for CS_2) we find that P_{th} is equal to 9 kW. For other organic liquids the minimum power is approximately 10 times larger.

9.3.3 Transient and Dynamical Features of SBS

The phonon lifetime for stimulated Brillouin scattering in liquids is of the order of several nanoseconds. Since Q-switched laser pulses have a duration of the order of several nanoseconds, and mode-locked laser pulses can be much shorter, it is normal for experiments on SBS to be performed in the transient regime. The nature of transient SBS has been treated by Kroll (1965), by Pohl et al. (1968), and by Pohl and Kaiser (1970).

The SBS equations can be solved including the transient nature of the phonon field. This was done first by Carman et al. (1970) and the results have been summarized by Zel'dovich et al. (1985). One finds that

$$I_S(L,T) \simeq \begin{cases} I_N \exp(-2\Gamma_B T + 2\sqrt{2(gIL)(\Gamma_B T)}\,) & \Gamma_B T < gIL/2, \\ I_N \exp(gIL) & \Gamma_B T > gIL/2. \end{cases} \tag{9.3.39}$$

Here I_N is the effective noise input that initiates the SBS process, gIL is the usual single pass gain, Γ_B is the phonon damping rate, and T is the laser pulse duration.

We can use this result to predict how the SBS threshold intensity I_{th} is increased through use of a short laser pulse. We require that in either limit given above the single pass amplification must equal the threshold value, which we take to be exp (25). We then find that

$$gI_{\text{th}}l = \begin{cases} (12.5 + \Gamma_B T)^2/2\Gamma_B T & \Gamma_B T < 12.5, \\ 25 & \Gamma_B T > 12.5. \end{cases} \tag{9.3.40}$$

This functional dependence is illustrated in Fig. 9.3.6. Note that even for laser pulses as long as twice the phonon lifetime, the threshold for SBS is raised by a factor of approximately two.

The SBS process is characterized by several different time scales, including the transit time of light through the interaction region, the laser pulse duration, and the phonon lifetime. Consequently, the SBS process can display quite rich dynamical effects. One of these effects is pulse

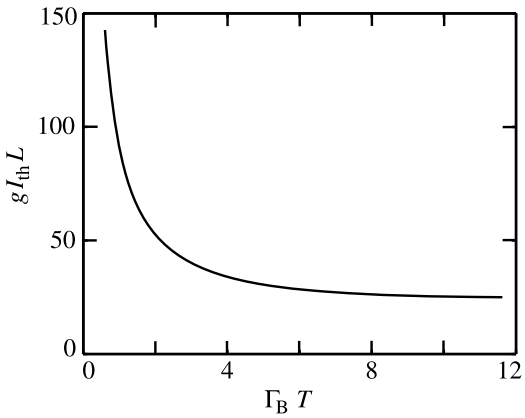

FIGURE 9.3.6: Dependence of the SBS threshold intensity I_{th} on the laser pulse duration T.

compression, the tendency of the SBS Stokes pulse to be shorter (at times very much shorter) than the incident laser pulse. This process is described in Problem 5 at the end of this chapter. When SBS is excited by a multi-longitudinal-mode laser, new types of dynamical behavior can occur. Here the various laser modes beat together leading to modulation in time of the laser intensity within the interaction region. This situation has been analyzed by Narum et al. (1986). In addition, the stochastic properties of SBS have been studied in considerable detail. SBS is initiated by noise in the form of thermally excited phonons. Since the SBS process involves nonlinear amplification (nonlinear because of pump depletion effects) in a medium with an effectively nonlocal response (nonlocal because the Stokes and laser fields are counterpropagating), the stochastic properties of the SBS output can be quite different from those of the phonon noise field that initiates SBS. These properties have been studied, for instance, by Gaeta and Boyd (1991). In addition, when SBS is excited by two counterpropagating pump fields, it can display even more complex behavior, including instability and chaos, as studied by Narum et al. (1988), Gaeta et al. (1989), and Kulagin et al. (1991).

9.4 Phase Conjugation by Stimulated Brillouin Scattering

It was noted even in the earliest experiments on stimulated Brillouin scattering (SBS) that the Stokes radiation was emitted in a highly collimated beam in the backward direction. In fact, the Stokes radiation was found to be so well collimated that it was efficiently fed back into the exciting laser, often leading to the generation of new spectral components in the output of the laser (Goldblatt and Hercher, 1968). These effects were initially explained as a purely geometrical effect resulting from the long but thin shape of the interaction region.

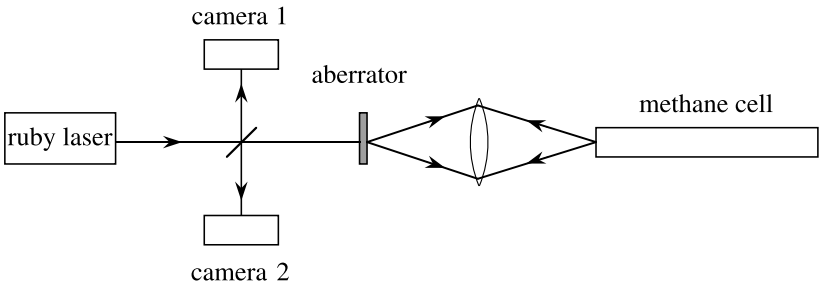

FIGURE 9.4.1: Setup of first experiment on phase conjugation by stimulated Brillouin scattering.

The first indication that the backscattered light was in fact the phase conjugate of the input was provided by an experiment of Zel'dovich et al. (1972). The setup used in this experiment is shown in Fig. 9.4.1. The output of a single-mode ruby laser was focused into a cell containing methane gas at a pressure of 125 atmospheres. This cell was constructed in the shape of a cylindrical, multimode waveguide and served to confine the radiation in the transverse dimension. A strong SBS signal was generated from within this cell. A glass plate that had been etched in hydrofluoric acid was placed in the incident beam to serve as an aberrator. Two cameras were used to monitor the transverse intensity distributions of the incident laser beam and of the Stokes return.

The results of this experiment are summarized in photographs taken by V.V. Ragulsky that are reproduced in Fig. 9.4.2. Part (a) of this figure shows the laser beam shape as recorded by camera 1, and part (b) shows the Stokes beam shape as recorded by camera 2. The similarity of the spot sizes and shapes indicates that the return beam is the phase conjugate of the incident beam. These highly elongated beam shapes are a consequence of the unusual mode pattern of the laser used in these experiments. Part (c) of the figure shows the spot size recorded by camera 2 when the SBS cell had been replaced by a conventional mirror. The spot size in this case is very much larger than that of the incident beam; this result shows the severity of the distortions impressed on the beam by the aberrator. Part (d) of the figure shows the spot size of the return beam when the aberrator was removed from the beam path. This spot size is larger than that shown in part (b). This result shows that SBS forms a more accurate conjugate of the incident light when the beam is highly distorted than when the beam is undistorted.*

The results of the experiment of Zel'dovich et al. are somewhat surprising, because it is not clear from inspection of the coupled-amplitude equations that describe the SBS process why SBS should lead to phase conjugation. We recall that the reason why degenerate four-wave mixing leads to phase conjugation is that the source term driving the output wave A_4 in the

* The conclusion that SBS forms a better phase conjugate of an aberrated beam than of an unaberrated beam is not true in all cases, and appears to be a consequence of the details of the geometry of the experiment of Zel'dovich et al.

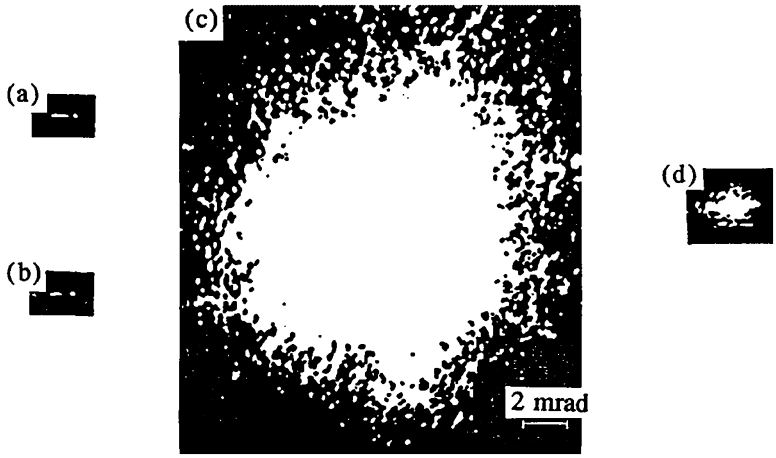

FIGURE 9.4.2: Results of the first experiment demonstrating SBS phase conjugation.

coupled-amplitude equations describing four-wave mixing (see, for example, Eq. (7.2.31b)) is proportional to the complex conjugate of the input wave amplitude, that is, to A_3^*. However, for the case of SBS, Eq. (9.3.21b) shows that the output wave amplitude A_2 is driven by a term proportional to $|A_1|^2 A_2$, which contains no information regarding the phase of the input wave A_1.

The reason why SBS leads to the generation of a phase-conjugate wave is in fact rather subtle and has been described by Zel'dovich et al. (1972) and by Sidorovich (1976). As illustrated in Fig. 9.4.3, we consider a badly aberrated optical wave that is focused into the SBS interaction region. Since the wave is highly aberrated, a highly nonuniform intensity distribution (i.e., a volume speckle pattern) is created in the focal region of the wave. Since the gain experienced by the Stokes wave depends on the local value of the laser intensity (see, for example, Eq. (9.3.22b)), a nonuniform gain distribution for the Stokes wave is therefore present in the focal volume. We recall that SBS is initiated by noise—that is, by spontaneously generated Stokes photons. The noise field that leads to SBS initially contains all possible spatial Fourier components. However, the portion of the noise field that experiences the maximum amplification is the portion whose intensity distribution best matches the nonuniform gain distribution. This portion of the noise field must have wavefronts that match those of the incident laser beam, and thus corresponds to the phase conjugate of the incident laser field.

In order to make this argument more precise, we consider the intensity equation satisfied by the Stokes field (see also Eq. (9.3.22b)),

$$\frac{dI_S}{dz} = -gI_L I_S. \tag{9.4.1}$$

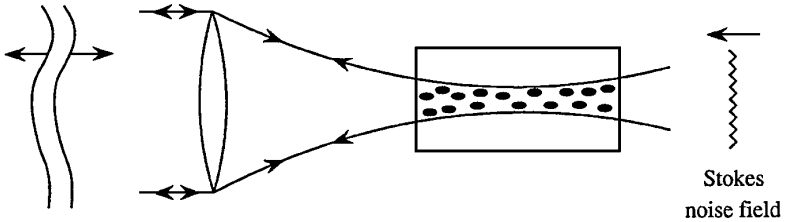

FIGURE 9.4.3: Origin of phase conjugation by SBS. The highly aberrated incident wavefront produces a highly nonuniform intensity distribution (and thus a nonuniform gain distribution) in the focal region of the lens.

Since we are now considering the case where I_L and I_S possess nonuniform transverse distributions, it is useful to consider the total power in each wave (at fixed z), defined by

$$P_L = \int I_L \, dA, \qquad P_S = \int I_S \, dA, \tag{9.4.2}$$

where the integrals are to be carried out over an area large enough to include essentially all of the power contained in each beam. Eq. (9.4.1) can then be rewritten in the form

$$\frac{dP_S}{dz} = -g\frac{P_L P_S}{A}C, \tag{9.4.3}$$

where $A = \int dA$ and where

$$C = \frac{\langle I_L I_S \rangle}{\langle I_L \rangle \langle I_S \rangle} \tag{9.4.4}$$

represents the normalized spatial cross-correlation function of the laser and Stokes field intensity distributions. Here the angular brackets are defined so that $\langle x \rangle = \int x \, dA/A$, where x denotes I_L, I_S, or the product $I_L I_S$.

We see that the power gain experienced by the Stokes wave depends not only on the total power of the laser wave, but also on the degree of correlation between the laser and Stokes wave intensity distributions. If I_L and I_S are completely uncorrelated, so that $\langle I_L I_S \rangle = \langle I_L \rangle \langle I_S \rangle$, the correlation function C takes on the value unity. C is equal to unity also for the case in which both I_L and I_S are spatially uniform. However, if I_L and I_S are correlated, for example, because the laser and Stokes fields are phase conjugates of one another, the correlation function can be greater than unity.

A limiting case is that in which the laser field is so badly aberrated that the transverse variations in the complex field amplitude obey gaussian statistics. In such a case, the probability density function for the laser intensity is given by (see, for example, Goodman, 1985)

$$P(I) = \frac{1}{I_0} e^{-I/I_0}. \tag{9.4.5}$$

The moments of this distribution are given in general by $\langle I^n \rangle = n \langle I \rangle^n$, and in particular the second moment is given by

$$\langle I^2 \rangle = 2 \langle I \rangle^2. \tag{9.4.6}$$

For that portion of the Stokes field that is the phase conjugate of the laser field, the intensity I_S will be proportional to I_L, and we see from Eqs. (9.4.4) and (9.4.6) that C will be equal to 2. Hence, the exponential gain $G \equiv g P_L C L / A$ experienced by the phase-conjugate portion of the noise field will be two times larger than that experienced by any other mode of the noise field. Since the threshold for SBS corresponds to G of the order of 30, the phase-conjugate portion of the SBS signal at threshold will be approximately exp (15) times larger than that of any other component.

On the basis of the argument just presented, we expect that high-quality phase conjugation will occur only if a large number of speckles of the laser intensity distribution are present within the interaction volume. We now determine the conditions under which the number of speckles will be large. We assume that in the focal region the incident laser field has transverse wavefront irregularities on a distance scale as small as a. Each such region will diffract the incident beam into a cone with a characteristic angular spread of $\theta = \lambda / a$. Hence, the speckle pattern will look appreciably different after the beam has propagated through the longitudinal distance Δz such that $\theta \Delta z = a$. These considerations show that $\Delta z = a^2 / \lambda$. We hence expect that SBS will lead to a high-quality phase-conjugate signal only if the transverse extent of the interaction region is much larger than a and if the longitudinal extent of the interaction region is much longer than Δz. In addition, the quality of the phase-conjugate signal can be degraded if there is poor spatial overlap of the various spatial Fourier components of the laser beam. For example, a highly aberrated beam will spread with a large angular divergence $\theta = \lambda / a$. If those components of the beam with large divergence angle θ fail to overlap the strong central portion of the beam, they will be reflected with low efficiency, leading to a degradation of the quality of the phase-conjugation process. To avoid the possibility of such effects, SBS phase conjugation is often performed using the waveguide geometry shown in Fig. 9.4.1.

One of the applications of SBS phase conjugation is in the design of high-power laser systems. Phase conjugation can be used to correct for aberrations caused, for instance, by thermal stresses induced in the laser gain medium; see, for example, Zakharenkov et al. (2007), and Bowers et al. (1997).

9.5 Stimulated Brillouin Scattering in Gases

We next consider stimulated Brillouin scattering (SBS) in gases. We saw above (Eq. (9.3.24)) that the steady-state line-center gain factor for SBS is given by

$$g_0 = \frac{\gamma_e^2 \omega^2}{\rho_0 n v c^3 \Gamma_B}, \tag{9.5.1}$$

with the electrostrictive constant γ_e given by Eq. (8.3.12) and with the Brillouin linewidth given to good approximation by (see also Eqs. (8.3.23) and (9.3.14b))

$$\Gamma_B = (2\eta_s + \eta_d)\, q^2/\rho_0. \tag{9.5.2}$$

For the case of an ideal gas, we can readily predict the values of the material parameters appearing in these equations (Loeb, 1961). First, we can assume the validity of the Stokes relation (see also the discussion in Appendix Section 9.6.1), which states that the shear and dilation viscosity coefficients are related by $\eta_d = -\frac{2}{3}\eta_s$, and we thus find that

$$\Gamma_B = \tfrac{4}{3}\eta_s q^2/\rho_0. \tag{9.5.3}$$

The shear viscosity coefficient η_s can be shown from kinetic theory to be given by

$$\eta_s = \tfrac{1}{3} N m \bar{v} L, \tag{9.5.4}$$

where N is the atomic number density, m is the molecular mass, $\bar{v}$ is the mean molecular velocity given by $\bar{v} = (8kT/\pi m)^{1/2}$, and L is the mean free path given by $L = (\sqrt{2}\pi d^2 N)^{-1}$ with d denoting the molecular diameter. We hence find that the shear viscosity coefficient is given by

$$\eta_s = \frac{2}{3\pi^{3/2}} \frac{\sqrt{kTm}}{d^2}. \tag{9.5.5}$$

Note that the shear viscosity coefficient is independent of the molecular number density N. The measured (and theoretical) value of the shear viscosity coefficient for nitrogen gas at standard temperature and pressure is $\eta_s = 1.8 \times 10^{-5}$ N s/m^2.

By introducing expression (9.5.5) for the viscosity into Eq. (9.5.2) and replacing q by $2n\omega/c$, we find that the Brillouin linewidth is given by

$$\Gamma_B = \frac{32}{9\pi^{3/2}} \frac{n^2\omega^2}{c^2} \frac{\sqrt{kT/m}}{d^2 N}. \tag{9.5.6}$$

If we assume that the incident optical radiation has a wavelength λ of 1.06 μm, we find that the Brillouin linewidth for nitrogen at standard temperature and pressure is equal to $\Gamma_B = 2.77 \times 10^9$ rad/sec and thus that the Brillouin linewidth in ordinary frequency units is given by $\delta\nu(\text{FWHM}) = \Gamma_B/2\pi = 440$ MHz.

The velocity of sound v, which appears in Eq. (9.5.1), is given for an ideal gas by $v = (\gamma kT/m)^{1/2}$, where γ, the ratio of specific heats, is equal to 5/3 for a monatomic gas and 7/5 for a diatomic gas. In addition, the electrostrictive constant γ_e can be estimated as $\gamma_e = \rho(\partial\epsilon/\partial\rho)$ with $(\partial\epsilon/\partial\rho)$ taken as the essentially constant quantity $(\epsilon - 1)/\rho$.

The dependence of g_0 on material parameters can be determined by combining these results with Eq. (9.5.1) to obtain

$$g_0 = \frac{9\pi^{3/2}N^2m^2d^2(\partial\epsilon/\partial\rho)^2}{32\gamma^{1/2}n^3ckT}. \tag{9.5.7}$$

However, in order to obtain a numerical estimate of g_0, it is often more convenient to evaluate the expression (9.5.1) for g_0 directly with the numerical value of Γ_B obtained from Eq. (9.5.6). For N_2 gas at standard temperature and pressure and for a wavelength of 1.06 μm, we take the values $\omega = 1.8 \times 10^{15}$ rad/sec, $n = 1.0003$, $v = 330$ m/sec, $\gamma_e = n^2 - 1 = 6 \times 10^{-4}$, and we thereby obtain

$$g_0 = 0.038\frac{\text{m}}{\text{TW}}. \tag{9.5.8}$$

Note from Eq. (9.5.7) that g_0 scales quadratically with molecular density. Hence, at a pressure of 100 atmospheres the gain factor of N_2 is equal to $g_0 = 0.38$ m/GW, which is comparable to that of typical organic liquids.

One advantage of the use of gases as the active medium for Brillouin scattering is that the gain for SBS scales with molecular number density as N^2, whereas the gain for stimulated Raman scattering, which is often a competing process, scales as N (see, for example, Eqs. (10.3.19) through (10.3.21) and (9.3.20)). At pressures greater than 10 atmospheres, the gain for SBS typically exceeds that of stimulated Raman scattering. Moreover, through the use of rare gases (which have no vibrational modes), it is possible to suppress the occurrence of stimulated Raman scattering altogether.

Some parameters relevant to SBS at the 249 nm wavelength of the KrF laser have been compiled by Damzen and Hutchinson (1983) and are presented in Table 9.5.1.

9.6 General Theory of Stimulated Brillouin and Stimulated Rayleigh Scattering

In this section we develop a theoretical model that can treat both stimulated Brillouin and stimulated Rayleigh scattering. These two effects can conveniently be treated together because they both entail the scattering of light from inhomogeneities in thermodynamic quantities. For convenience, we choose the temperature T and density ρ to be the independent thermodynamic variables. The theory that we present incorporates both electrostrictive and absorptive coupling of the radiation to the material system. Our analysis therefore describes the following four scattering processes:

1. *Electrostrictive stimulated Brillouin scattering.* The scattering of light from sound waves that are driven by the interference of the laser and Stokes fields through the process of electrostriction.

TABLE 9.5.1: Gain factors, phonon lifetimes, and frequency shifts for some compressed Brillouin-active gases at a wavelength of 249 nm[a].

Gas	p (atm)	g_0 (m/GW)	τ (nsec)	$\Omega_B/2\pi$ (GHz)	g_R (m/GW)
SF_6	15.5	2.5×10^{-1}	1	0.9	3×10^{-3}
	10	0.9×10^{-1}	0.6		2×10^{-3}
Xe	39	4.4×10^{-1}	2	1.4	0
	10	1.8×10^{-2}	0.4		
Ar	10	1.5×10^{-3}	0.1	3	0
N_2	10	1.7×10^{-3}	0.2	3	3×10^{-4}
CH_4	10	8×10^{-3}	0.1	3	1×10^{-2}

[a] For comparison, the gain factor g_R for forward stimulated Raman scattering is also listed. (After Damzen and Hutchinson, 1983.)

2. *Thermal stimulated Brillouin scattering.* The scattering of light from sound waves that are driven by the absorption and subsequent thermalization of the optical energy, leading to temperature and hence to density variations within the medium.
3. *Electrostrictive stimulated Rayleigh scattering.* The scattering of light from isobaric density fluctuations that are driven by the process of electrostriction.
4. *Thermal stimulated Rayleigh scattering.* The scattering of light from isobaric density fluctuations that are driven by the process of optical absorption.

Our analysis is based on the three equations of hydrodynamics (Hunt, 1955; Kaiser and Maier, 1972). The first of these equations is the equation of continuity

$$\frac{\partial \tilde{\rho}_t}{\partial t} + \tilde{\mathbf{u}}_t \cdot \nabla \tilde{\rho}_t + \tilde{\rho}_t \nabla \cdot \tilde{\mathbf{u}}_t = 0, \tag{9.6.1}$$

where $\tilde{\rho}_t$ is the mass density of the fluid and $\tilde{\mathbf{u}}_t$ is the velocity of some small volume element of the fluid.* The second equation is the equation of momentum transfer. It is a generalization of the Navier–Stokes equation and is given by

$$\tilde{\rho}_t \frac{\partial \tilde{\mathbf{u}}_t}{\partial t} + \tilde{\rho}_t (\tilde{\mathbf{u}}_t \cdot \nabla)\tilde{\mathbf{u}}_t = \tilde{\mathbf{f}} - \nabla \tilde{p}_t + (2\eta_s + \eta_d)\nabla(\nabla \cdot \tilde{\mathbf{u}}_t) - \eta_s \nabla \times (\nabla \times \tilde{\mathbf{u}}_t). \tag{9.6.2}$$

Here $\tilde{\mathbf{f}}$ represents the force per unit volume of any externally imposed forces; for the case of electrostriction, $\tilde{\mathbf{f}}$ is given by (see also Eq. (9.3.12))

$$\tilde{\mathbf{f}} = -\tfrac{1}{2}\epsilon_0 \gamma_e \nabla \langle \tilde{\mathbf{E}} \cdot \tilde{\mathbf{E}} \rangle, \tag{9.6.3}$$

* The subscript t stands for *total*; we shall later linearize these equations to find the equations satisfied by the linearized quantities, which we shall designate by nonsubscripted symbols.

where $\tilde{\mathbf{E}}$ denotes the instantaneous value of the time-varying applied total electric field and γ_e represents the electrostrictive coupling constant

$$\gamma_e = \rho \frac{\partial \epsilon}{\partial \rho}. \tag{9.6.4}$$

The second term on the right-hand side of Eq. (9.6.2) denotes the force due to the gradient of the pressure $\tilde{p}_t$. In the third term, η_s denotes the shear viscosity coefficient and η_d denotes the dilational viscosity coefficient. When the Stokes relation is satisfied, as it is for example for an ideal gas, these coefficients are related by

$$\eta_d = -\tfrac{2}{3}\eta_s. \tag{9.6.5}$$

The coefficients are defined in detail in the Appendix at the end of this section.

The last of three principal equations of hydrodynamics is the equation of heat transport, given by

$$\tilde{\rho}_t C_v \frac{\partial \tilde{T}_t}{\partial t} + \tilde{\rho}_t c_v (\tilde{\mathbf{u}} \cdot \nabla \tilde{T}_t) + \tilde{\rho}_t c_v \left(\frac{\gamma - 1}{\beta_p} \right) (\nabla \cdot \tilde{\mathbf{u}}_t) = -\nabla \cdot \tilde{\mathbf{Q}} + \tilde{\phi}_\eta + \tilde{\phi}_{\text{ext}}. \tag{9.6.6}$$

Here $\tilde{T}_t$ denotes the local value of the temperature, c_v the specific heat at constant volume, $\gamma = c_p/c_v$ the adiabatic index, $\beta_p = -\tilde{\rho}^{-1}(\partial \tilde{\rho}/\partial \tilde{T})_p$ the thermal expansion coefficient, and $\tilde{\mathbf{Q}}$ the heat flux vector. For heat flow due to thermal conduction, $\tilde{\mathbf{Q}}$ satisfies the equation

$$\nabla \cdot \tilde{\mathbf{Q}} = -\kappa \nabla^2 \tilde{T}_t, \tag{9.6.7}$$

where κ denotes the thermal conductivity. $\tilde{\phi}_\eta$ denotes the viscous energy deposited within the medium per unit volume per unit time and is given by

$$\tilde{\phi}_\eta = \sum_{ij} (2\eta_s d_{ij} d_{ji} + \eta_d d_{ii} d_{jj}), \tag{9.6.8a}$$

where

$$d_{ij} = \frac{1}{2} \left(\frac{\partial \tilde{u}_i}{\partial x_j} + \frac{\partial \tilde{u}_j}{\partial x_i} \right) \tag{9.6.8b}$$

is the rate-of-dilation tensor. Finally, $\tilde{\phi}_{\text{ext}}$ gives the energy per unit time per unit volume delivered to the medium from external sources. Absorption of the optical wave provides the contribution

$$\tilde{\phi}_{\text{ext}} = \alpha n \epsilon_0 c \langle \tilde{E}^2 \rangle, \tag{9.6.9}$$

to this quantity, where α is the optical absorption coefficient.

The acoustic equations are now derived by linearizing the hydrodynamic equations about the nominal conditions of the medium. In particular, we take

$$\tilde{\rho}_t = \rho_0 + \tilde{\rho} \quad \text{with} \quad |\tilde{\rho}| \ll \rho_0, \tag{9.6.10a}$$

$$\tilde{T}_t = T_0 + \tilde{T} \quad \text{with} \quad |\tilde{T}| \ll T_0, \tag{9.6.10b}$$

$$\tilde{\mathbf{u}}_t = \tilde{\mathbf{u}} \quad \text{with} \quad |\tilde{\mathbf{u}}| \ll v, \tag{9.6.10c}$$

where v denotes the velocity of sound. Note that we have assumed that the medium is everywhere motionless in the absence of the acoustic disturbance. We can reliably use the linearized form of the resulting equations so long as the indicated inequalities are satisfied.

We substitute the expansions (9.6.10) into the hydrodynamic equations (9.6.1), (9.6.2), and (9.6.6), drop any term that contains more than one small quantity, and subtract the unperturbed, undriven solution containing only $\tilde{\rho}_0$ and $\tilde{T}_0$. The continuity equation (9.6.1) then becomes

$$\frac{\partial \tilde{\rho}}{\partial t} + \rho_0 \nabla \cdot \tilde{\mathbf{u}} = 0. \tag{9.6.11}$$

In order to linearize the momentum transport equation (9.6.2), we first express the total pressure $\tilde{p}_t$ as

$$\tilde{p}_t = p_0 + \tilde{p} \quad \text{with} \quad |\tilde{p}| \ll p_0. \tag{9.6.12}$$

Since we have taken T and ρ as the independent thermodynamic variables, we can express $\tilde{p}$ as

$$\tilde{p} = \left(\frac{\partial p}{\partial \rho}\right)_T \tilde{\rho} + \left(\frac{\partial p}{\partial T}\right)_\rho \tilde{T} \tag{9.6.13}$$

or as

$$\tilde{p} = \frac{v^2}{\gamma}(\tilde{\rho} + \beta_p \rho_0 \tilde{T}), \tag{9.6.14}$$

where we have expressed $(\partial p/\partial \rho)_T$ as $\gamma^{-1}(\partial p/\partial \rho)_s = v^2/\gamma$ with $v^2 = (\partial p/\partial \rho)_s$ representing the square of the velocity of sound, and where we have expressed $(\partial p/\partial T)_\rho$ as $\gamma^{-1}(\partial p/\partial \rho)_s(\partial \rho/\partial T)_p = v^2 \beta_p \rho_0/\gamma$ with β_p representing the thermal expansion coefficient at constant pressure. Through use of Eq. (9.6.14), the linearized form of Eq. (9.6.2) becomes

$$\rho_0 \frac{\partial \tilde{\mathbf{u}}}{\partial t} + \frac{v^2}{\gamma}\nabla \tilde{\rho} + \frac{v^2 \beta_p \rho_0}{\gamma}\nabla \tilde{T} - (2\eta_s + \eta_d)\nabla(\nabla \cdot \tilde{\mathbf{u}}) + \eta_s \nabla \times (\nabla \times \tilde{\mathbf{u}}) = \tilde{\mathbf{f}}. \tag{9.6.15}$$

Finally, the linearized form of the energy transport equation, Eq. (9.6.6), becomes

$$\rho_0 c_v \frac{\partial \tilde{T}}{\partial t} + \frac{\rho_0 c_v (\gamma - 1)}{\beta_p}(\nabla \cdot \tilde{\mathbf{u}}) - \kappa \nabla^2 \tilde{T} = \tilde{\phi}_{\text{ext}}. \tag{9.6.16}$$

Note that the viscous contribution to the heat input, $\tilde{\phi}_\eta$, does not contribute in the linear approximation.

Eqs. (9.6.11), (9.6.15), and (9.6.16) constitute the three linearized equations of hydrodynamics for the quantities $\tilde{\mathbf{u}}$, $\tilde{\rho}$, and $\tilde{T}$. The continuity equation in its linearized form (Eq. (9.6.11)) can be used to eliminate the variable $\tilde{\mathbf{u}}$ from the remaining two equations. To do so, we take the divergence of the equation of momentum transfer (9.6.15) and use Eq. (9.6.11) to eliminate the terms containing $\nabla \cdot \tilde{\mathbf{u}}$. We obtain

$$-\frac{\partial^2 \tilde{\rho}}{\partial t^2} + \frac{v^2}{\gamma}\nabla^2\tilde{\rho} + \frac{v^2\beta_p\rho_0}{\gamma}\nabla^2\tilde{T} + \frac{2\eta_s + \eta_d}{\rho_0}\frac{\partial}{\partial t}\left(\nabla^2\tilde{\rho}\right) = \tfrac{1}{2}\epsilon_0\gamma_e\nabla^2\left\langle\tilde{E}^2\right\rangle, \tag{9.6.17}$$

where we have explicitly introduced the form of $\tilde{\mathbf{f}}$ from Eq. (9.6.3). Also, the energy transport equation (9.6.16) can then be expressed through use of Eqs. (9.6.9) and (9.6.11) as

$$\rho_0 c_v\frac{\partial\tilde{T}}{\partial t} - \frac{c_v(\gamma-1)}{\beta_p}\frac{\partial\tilde{\rho}}{\partial t} - \kappa\nabla^2\tilde{T} = n\epsilon_0 c\alpha\left\langle\tilde{E}^2\right\rangle. \tag{9.6.18}$$

Eqs. (9.6.17) and (9.6.18) constitute two coupled equations for the thermodynamic variables $\tilde{\rho}$ and $\tilde{T}$, and they show how these quantities are coupled to one another and are driven by the applied optical field.

In the absence of the driving terms appearing on their right-hand sides, Eqs. (9.6.17) and (9.6.18) allow solutions of the form of damped, freely propagating acoustic waves

$$\tilde{F}(z,t) = Fe^{-i\Omega(t-z/v)}e^{-\alpha_s z} + \text{c.c.}, \tag{9.6.19}$$

where F denotes either ρ or T, and where the sound absorption coefficient α_s is given for low frequencies ($\Omega \ll \rho_0 v^2/(2\eta_s + \eta_d)$) by

$$\alpha_s = \frac{\Omega^2}{2\rho_0 v^3}\left[(2\eta_s + \eta_d) + (\gamma-1)\frac{\kappa}{c_p}\right]. \tag{9.6.20}$$

For details, see the article by Sette (1961).

We next study the nature of the solution to Eqs. (9.6.17) and (9.6.18) in the presence of their driving terms. We assume that the total optical field can be represented as

$$\tilde{E}(z,t) = A_1 e^{i(k_1 z - \omega_1 t)} + A_2 e^{i(-k_2 z - \omega_2 t)} + \text{c.c.} \tag{9.6.21}$$

We first determine the response of the medium at the beat frequency between these two applied field frequencies. This disturbance will have frequency

$$\Omega = \omega_1 - \omega_2 \tag{9.6.22}$$

and wavenumber

$$q = k_1 + k_2 \tag{9.6.23}$$

and can be taken to be of the form

$$\tilde{\rho}(z,t) = \rho e^{i(qz-\Omega t)} + \text{c.c.}, \tag{9.6.24}$$

$$\tilde{T}(z,t) = T e^{i(qz-\Omega t)} + \text{c.c.} \tag{9.6.25}$$

For the present, we are interested only in the steady-state response of the medium, and thus we assume that the amplitudes A_1, A_2, ρ, and T are time-independent. We introduce the fields $\tilde{E}$, $\tilde{\rho}$, and $\tilde{T}$ given by Eqs. (9.6.21) through (9.6.25) into the coupled acoustic equations (9.6.17) and (9.6.18). The parts of these equations that oscillate at frequency Ω are given respectively by

$$-\left(\Omega^2 + i\Omega\Gamma_{\text{B}} - \frac{v^2q^2}{\gamma}\right)\rho + \frac{v^2\beta_p\rho_0 q^2}{\gamma}T = \epsilon_0\gamma_e q^2 A_1 A_2^* \tag{9.6.26}$$

and

$$-\left(i\Omega - \frac{1}{2}\gamma\Gamma_R\right)T + \frac{i(\gamma-1)\Omega}{\beta_p\rho_0}\rho = \frac{2n\epsilon_0 c\alpha}{c_v\rho_0}A_1A_2^*. \tag{9.6.27}$$

Here we have introduced the Brillouin linewidth

$$\Gamma_{\text{B}} = (2\eta_s + \eta_d)q^2/\rho_0, \tag{9.6.28}$$

whose reciprocal $\tau_p = \Gamma_{\text{B}}^{-1}$ is the phonon lifetime, and the Rayleigh linewidth

$$\Gamma_R = \frac{2\kappa q^2}{\rho_0 c_p}, \tag{9.6.29}$$

whose reciprocal $\tau_R = \Gamma_R^{-1}$ is characteristic decay time of the isobaric density disturbances that give rise to Rayleigh scattering.

In deriving Eqs. (9.6.26) and (9.6.27) we have ignored those terms that contain the spatial derivatives of ρ and T. This approximation is equivalent to assuming that the material excitations are strongly damped and hence do not propagate over any appreciable distances. This approximation is valid so long as

$$q \gg \left|\frac{1}{\rho}\frac{\partial\rho}{\partial z}\right| \left|\frac{1}{T}\frac{\partial T}{\partial z}\right| \quad \text{and} \quad q^2 \gg \left|\frac{1}{\rho}\frac{\partial^2\rho}{\partial z^2}\right| \left|\frac{1}{T}\frac{\partial^2 T}{\partial z^2}\right|.$$

These inequalities are usually satisfied. Recall that a similar approximation was introduced in Section 9.3 in the derivation of Eq. (9.3.15).

We next solve Eq. (9.6.27) algebraically for T and introduce the resulting expression into Eq. (9.6.26). We obtain the equation

$$\left[-\left(\Omega^2 + i\Omega\Gamma_{\mathrm{B}} - \frac{v^2q^2}{\gamma}\right) + \frac{v^2q^2\Omega(\gamma-1)}{\left(\Omega + \frac{1}{2}i\gamma\Gamma_R\right)\gamma}\right]\rho = \left[\epsilon_0\gamma_e - \frac{i\gamma_a q v}{\Omega + \frac{1}{2}i\gamma\Gamma_R}\right]q^2A_1A_2^*, \tag{9.6.30}$$

where we have introduced the absorptive coupling constant

$$\gamma_a = \frac{8\pi\alpha n v^2\epsilon_0 c\beta_p}{c_P\Omega_{\mathrm{B}}} \tag{9.6.31}$$

with $\Omega_{\mathrm{B}} = qv$. Eq. (9.6.30) shows how the amplitude ρ of the acoustic disturbance depends on the amplitudes A_1 and A_2 of the two optical fields. Both Brillouin and Rayleigh contributions to ρ are contained in Eq. (9.6.30).

It is an empirical fact (see, for example, Fig. 8.1.1) that the spectrum for Brillouin scattering does not appreciably overlap that for Rayleigh scattering. Eq. (9.6.30) can thus be simplified by considering the resonant contributions to the two processes separately. First, we consider the case of stimulated Brillouin scattering (SBS). In this case Ω^2 is approximately equal to $\Omega_{\mathrm{B}}^2 = v^2q^2$, and thus the denominator $\Omega + \frac{1}{2}i\gamma\Gamma_R$ is nonresonant. We can thus drop the contribution $\frac{1}{2}i\gamma\Gamma_R$ in comparison with Ω in these denominators. Eq. (9.6.30) then shows that the Brillouin contribution to ρ is given by

$$\rho_{\mathrm{B}} = \frac{-(\epsilon_0\gamma_e - i\gamma_a)q^2}{4\pi(\Omega^2 + i\Omega\Gamma_{\mathrm{B}} - v^2q^2)}A_1A_2^*. \tag{9.6.32}$$

The other resonance in Eq. (9.6.30) occurs at $\Omega = 0$ and leads to stimulated Rayleigh scattering (SRLS). For $|\Omega| \lesssim \Gamma_R$, the Brillouin denominator $\Omega^2 + i\Omega\Gamma_{\mathrm{B}} - v^2q^2/\gamma$ is nonresonant and can be approximated by $-v^2q^2/\gamma$. Eq. (9.6.30) thus becomes

$$\rho_R = \left[\frac{\epsilon_0\gamma_e(\Omega + \frac{1}{2}i\gamma\Gamma_R) - i\gamma_a\Omega_{\mathrm{B}}}{\Omega + \frac{1}{2}i\Gamma_R}\right]\frac{1}{4\pi v^2}A_1A_2^*. \tag{9.6.33}$$

We next calculate the nonlinear polarization as

$$\tilde{p}^{\mathrm{NL}} = \epsilon_0\Delta\chi\tilde{E} = \epsilon_0\Delta\epsilon\tilde{E} = \epsilon_0\left(\frac{\partial\epsilon}{\partial\rho}\right)_T\tilde{\rho}\tilde{E} = \frac{\epsilon_0\gamma_e}{\rho_0}\tilde{\rho}\tilde{E}, \tag{9.6.34}$$

where $\tilde{\rho}$ and $\tilde{E}$ are given by Eqs. (9.6.24) and (9.6.21), respectively. We represent the nonlinear polarization in terms of its complex amplitudes as

$$\tilde{P}^{\mathrm{NL}} = p_1e^{i(k_1z-\omega_1t)} + p_2e^{i(-k_2z-\omega_2t)} + \text{c.c.} \tag{9.6.35}$$

with

$$p_1 = \frac{\epsilon_0 \gamma_e}{\rho_0} \rho A_2, \qquad p_2 = \frac{\epsilon_0 \gamma_e}{\rho_0} \rho^* A_1. \tag{9.6.36}$$

This form of the nonlinear polarization is now introduced into the wave equation, which we write in the form (see also Eq. (2.1.22))

$$\nabla^2 \left[A_n(\mathbf{r})\, e^{i\mathbf{k}_n \cdot \mathbf{r}} \right] + \frac{\epsilon(\omega_n)\omega_n^2}{c^2} A_n(\mathbf{r}) e^{i\mathbf{k}_n \cdot \mathbf{r}} = \frac{\omega_n^2}{\epsilon_0 c^2} p_n\, e^{i\mathbf{k}_n \cdot \mathbf{r}}. \tag{9.6.37}$$

We next make the slowly-varying amplitude approximation and find that the field amplitudes obey the equations

$$\left(\frac{d}{dz} + \tfrac{1}{2}\alpha \right) A_1 = \frac{i\omega}{2n\epsilon_0 c} p_1, \tag{9.6.38a}$$

$$\left(\frac{d}{dz} - \tfrac{1}{2}\alpha \right) A_2 = \frac{-i\omega}{2n\epsilon_0 c} p_2, \tag{9.6.38b}$$

where we have introduced the real part of the refractive index $n = \mathrm{Re}\,\sqrt{\epsilon}$ and the optical absorption coefficient $\alpha = (2\omega/c)\,\mathrm{Im}\,\sqrt{\epsilon}$. Eqs. (9.6.38) can be used to describe either SBS or SRLS, depending on whether form (9.6.32) or (9.6.33) is used to determine the factor ρ that appears in the expression (9.3.36) for the nonlinear polarization. Since in either case ρ is proportional to the product $A_1 A_2^*$, Eqs. (9.6.38) can be written as

$$\frac{dA_1}{dz} = \kappa |A_2|^2 A_1 - \tfrac{1}{2}\alpha A_1, \tag{9.6.39a}$$

$$\frac{dA_2}{dz} = \kappa^* |A_1|^2 A_2 + \tfrac{1}{2}\alpha A_2, \tag{9.6.39b}$$

where for SBS κ is given by

$$\kappa_{\mathrm{B}} = -\frac{q^2 \omega}{2\rho_0 n c} \frac{i\gamma_e(\epsilon_0 \gamma_e - i\gamma_a)}{(\Omega^2 + i\Omega\Gamma_{\mathrm{B}} - v^2 q^2)}, \tag{9.6.40a}$$

and for SRLS is given by

$$\kappa_R = \frac{i\gamma_e \omega}{2\rho_0 n c v^2} \left[\frac{\gamma_e\left(\Omega + \frac{1}{2} i\gamma\Gamma_R\right) - i\gamma_a \Omega_{\mathrm{B}}}{\Omega + \frac{1}{2} i\Gamma_R} \right]. \tag{9.6.40b}$$

We now introduce the intensities

$$I_i = 2n\epsilon_0 c |A_i|^2 \tag{9.6.41}$$

of the two interacting optical waves and use Eqs. (9.6.39) to calculate the spatial rate of change of the intensities as

$$\frac{dI_1}{dz} = -gI_1I_2 - \alpha I_1, \tag{9.6.42a}$$

$$\frac{dI_2}{dz} = -gI_1I_2 + \alpha I_2, \tag{9.6.42b}$$

where we have introduced the gain factor

$$g = -\frac{1}{n\epsilon_0 c}\,\mathrm{Re}\,\kappa. \tag{9.6.43}$$

For the case of SBS, we find that the gain factor can be expressed as

$$g_{\mathrm{B}} = g_{\mathrm{B}}^{e} + g_{\mathrm{B}}^{a}, \tag{9.6.44a}$$

where

$$g_{\mathrm{B}}^{e} = \frac{\omega^2\gamma_e^2}{\rho_0 n v c^2 \Gamma_{\mathrm{B}}}\,\frac{1}{1+(2\Delta\Omega/\Gamma_{\mathrm{B}})^2} \tag{9.6.44b}$$

and

$$g_{\mathrm{B}}^{a} = \frac{-\omega^2\gamma_e\gamma_a}{2\rho_0 n v c^2 \Gamma_{\mathrm{B}}}\,\frac{4\Delta\Omega/\Gamma_{\mathrm{B}}}{1+(2\Delta\Omega/\Gamma_{\mathrm{B}})^2} \tag{9.6.44c}$$

denote the electrostrictive and absorptive contributions to the SBS gain factor, respectively. Here we have introduced the detuning from the Brillouin resonance given by $\Delta\Omega = \Omega_{\mathrm{B}} - \Omega$, where $\Omega_{\mathrm{B}} = qv = (k_1 + k_2)v$ and where $\Omega = \omega_1 - \omega_2$. The electrostrictive contribution is maximum for $\Delta\Omega = 0$, where it attains the value

$$g_{\mathrm{B}}^{e}(\max) = \frac{\omega^2\gamma_e^2}{\rho_0 n v c^3 \Gamma_{\mathrm{B}}}. \tag{9.6.45}$$

Since (according to Eq. (9.6.28)) Γ_{B} is proportional to q^2 and thus to ω^2, the gain for electrostrictive SBS is independent of the laser frequency. The absorptive contribution is maximum for $\Delta\Omega = -\Gamma_{\mathrm{B}}/2$—that is, when the Stokes wave (at frequency ω_2) is detuned by one-half the spontaneous Brillouin linewidth Γ_{B} to the low-frequency side of resonance. The maximum value of the gain for this process is

$$g_{\mathrm{B}}^{a}(\max) = \frac{\omega^2\gamma_e\gamma_a}{2\rho_0 n v c^3 \Gamma_{\mathrm{B}}}. \tag{9.6.46}$$

Note that since Γ_{B} is proportional to q^2 and (according to Eq. (9.6.31)) γ_a is proportional to q^{-1}, the absorptive SBS gain factor is proportional to q^3 and hence depends on the laser

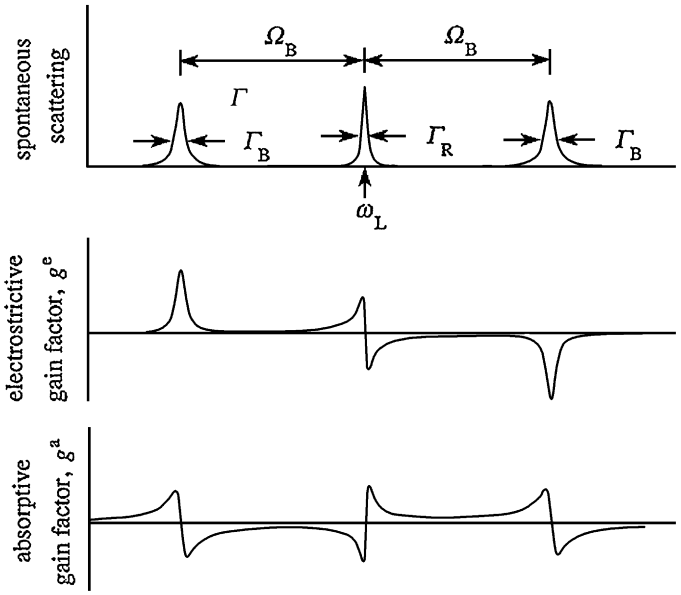

FIGURE 9.6.1: Gain spectra for stimulated Brillouin scattering and stimulated Rayleigh scattering, showing their electrostrictive and absorptive contributions. For comparison, the spectrum of spontaneous Brillouin and Rayleigh scattering is also shown.

frequency as ω^{-3}. Since the gain factor for thermal SBS is linearly proportional to the optical absorption coefficient α (by Eqs. (9.6.31) and (9.6.46)), the gain for thermal SBS can be made to exceed that for electrostrictive SBS by adding an absorber such as a dye to the Brillouin-active medium. As shown in Table 9.3.1, this effect occurs roughly for absorption coefficients greater than 1 cm^{-1}.*

The spectral dependence of the two contributions to the SBS gain is shown schematically in Fig. 9.6.1.

For the case of stimulated Rayleigh scattering, we can express the gain factor appearing in Eqs. (9.6.42) through use of Eqs. (9.6.40b) and (9.6.43) as

$$g_R = g_R^e + g_R^a, \tag{9.6.47}$$

where

$$g_R^e = \frac{-\omega\gamma_e^2(\gamma-1)}{4\rho_0 n^2 c^2 v^2}\left[\frac{4\Omega/\Gamma_R}{1+(2\Omega/\Gamma_R)^2}\right] \tag{9.6.48}$$

* The quantity $g_B^e(\text{max})$ is designated g_0 in Table 9.3.1.

TABLE 9.6.1: Properties of stimulated Rayleigh scattering for a variety of materials at a wavelength of 694 nm[a].

Substance	Gain factor		Linewidth
	g_e(max) (cm/MW)	g_a(max)/α (cm^2/MW)	$\delta\nu_R$ (MHz)
CCl_4	2.6×10^{-4}	0.82	17
Methanol	8.4×10^{-4}	0.32	20
CS_2	6.0×10^{-4}	0.62	36
Benzene	2.2×10^{-4}	0.57	24
Acetone	2.0×10^{-4}	0.47	21
H_2O	0.02×10^{-4}	0.019	27.5
Ethanol		0.38	18

[a] After Kaiser and Maier (1972).

and

$$g_R^a = \frac{\omega\gamma_e\gamma_a\Omega_B}{2\rho_0 n^2 c^2 v^2 \Gamma_R}\left[\frac{4\Omega/\Gamma_R}{1+(2\Omega/\Gamma_R)^2}\right] \tag{9.6.49}$$

denote the electrostrictive and absorptive contributions to the gain factor, respectively. The contribution g_R^e gives rise to electrostrictive stimulated Rayleigh scattering. The gain factor for this process is maximum for $\Omega = -\Gamma_R/2$ and has the value

$$g_R^e(\text{max}) = \frac{\omega\gamma_e^2(\gamma-1)}{4\rho_0 n^2 c^2 v^2}. \tag{9.6.50}$$

Note that this quantity scales linearly with laser frequency. The absorptive contribution g_R^a gives rise to thermal SRLS. The gain for this process is maximum for $\Omega = \Gamma_R/2$ and has the value

$$g_R^a(\text{max}) = \frac{\omega\gamma_e\gamma_a\Omega_B}{2\rho_0 n^2 c^2 v^2 \Gamma_R}. \tag{9.6.51}$$

Since Γ_R scales with the laser frequency as ω^2, γ_a scales as $1/\omega$, and Ω_B scales as ω, we see that the gain factor for thermal SRLS scales with the laser frequency as $1/\omega$.

As can be seen from Table 9.6.1, Γ_R is often of the order of 10 MHz, which is much narrower than the linewidths of pulsed lasers. In such cases, laser linewidth effects can often be treated in an approximate fashion by convolving the gain predicted by Eqs. (9.6.48) and (9.6.49) with the laser lineshape. If the laser linewidth Γ_L is much broader than Γ_R, the maximum gain for absorptive SRLS is then given by Eq. (9.6.51) with Γ_R replaced by Γ_L. Under these conditions g_R^a(max) is independent of the laser frequency.

We note by inspection of Table 9.6.1 that g_R^a(max) is very much larger than g_R^e(max) except for extremely small values of the absorption coefficient. The two gains become comparable for $\alpha \simeq 10^{-3}$ cm^{-1}, which occurs only for unusually pure materials.

We also see by comparison of Eqs. (9.6.51) and (9.6.46) that the ratio of the two thermal gain factors is given by

$$\frac{g_R^a(\max)}{g_B^a(\max)} = \frac{2\Gamma_B}{\Gamma_R}. \tag{9.6.52}$$

Comparison of Tables 9.3.1 and 9.6.1 shows that for a given material the ratio Γ_B/Γ_R is typically of the order of 100. Hence, when thermal stimulated scattering occurs, the gain for thermal SRLS is much larger than that for thermal SBS, and most of the energy is emitted by this process.

The frequency dependence of the gain for stimulated Rayleigh scattering is shown in Fig. 9.6.1. Note that electrostrictive SRLS gives rise to gain for Stokes shifted light but that thermal SRLS gives rise to gain for anti-Stokes scattering (Herman and Gray, 1967). This result can be understood from the point of view that n_2 is positive for electrostriction but is negative for the process of heating and subsequent thermal expansion. We saw in the discussion of two-beam coupling presented in Section 7.4 that the lower-frequency wave experiences gain for n_2 positive and loss for n_2 negative.

9.6.1 Appendix: Definition of the Viscosity Coefficients

The viscosity coefficients are defined as follows: The component t_{ij} of the stress tensor gives the i component of the force per unit area on an area element whose normal is in the j direction. We represent the stress tensor as

$$t_{ij} = -p\delta_{ij} + \sigma_{ij},$$

where p is the pressure and σ_{ij} is the contribution to the stress tensor due to viscosity. If we assume that σ_{ij} is linearly proportional to the rate of deformation

$$d_{ij} = \frac{1}{2}\left[\frac{\partial \tilde{u}_i}{\partial x_j} + \frac{\partial \tilde{u}_j}{\partial x_j}\right],$$

we can represent σ_{ij} as

$$\sigma_{ij} = 2\eta_s d_{ij} + \eta_d \delta_{ij} \sum_k d_{kk},$$

where η_s is the shear viscosity coefficient and η_d is the dilational viscosity coefficient. The quantity $\sum_k d_{kk}$ can be interpreted as follows:

$$\sum_k d_{kk} = \sum_k \frac{\partial \tilde{u}_k}{\partial x_k} = \nabla \cdot \tilde{\mathbf{u}}.$$

In general, η_s and η_d are independent parameters. However, for certain physical systems they are related to one another through a relationship first formulated by Stokes. This relationship results from the assumption that the viscous stress tensor σ_{ij} is traceless. In this case the trace of t_{ij} is unaffected by viscous effects; in other words, the mean pressure $-\frac{1}{3}\sum_i t_{ii}$ is unaffected by the effects of viscosity. Condition that σ_{ij} is traceless implies that the combination

$$\sum_i \sigma_{ii} = 2\eta_s \sum_i d_{ii} + 3\eta_d \sum_k d_{kk} = (2\eta_s + 3\eta_d) \sum_k d_{kk}$$

vanishes or that

$$\eta_d = -\tfrac{2}{3}\eta_s.$$

This result is known as the Stokes relation.

The viscosity coefficients η_s and η_d often appear in the combination $2\eta_s + \eta_d$, as they do in Eq. (9.6.2). When the Stokes relation is satisfied, this combination takes the value

$$2\eta_s + \eta_d = \tfrac{4}{3}\eta_s \quad \text{(Stokes relation valid)}.$$

Under general conditions, such that the Stokes relation is not satisfied, one often defines the bulk viscosity coefficient η_b by

$$\eta_b = \tfrac{2}{3}\eta_s + \eta_d,$$

in terms of which the quantity $2\eta_s + \eta_d$ can be represented as

$$2\eta_s + \eta_d = \tfrac{4}{3}\eta_s + \eta_b \quad \text{(in general)}.$$

Note that η_{B} vanishes identically when the Stokes relation is valid, for example, for the case of an ideal gas.

As an example of the use of these relations, we note that the Brillouin linewidth Γ_{B} introduced in Eqs. (8.3.23), (9.5.2), and (9.6.28) can be represented (ignoring the contribution due to thermal conduction) either as

$$\Gamma_{\mathrm{B}} = (2\eta_s + \eta_d)q^2/\rho_0$$

or as

$$\Gamma_{\mathrm{B}} = \left(\tfrac{4}{3}\eta_s + \eta_{\mathrm{B}}\right)q^2/\rho_0.$$

Problems

1. *Lorentz–Lorenz prediction of the electrostrictive constant.* Verify Eq. (9.2.17).
2. *Angular dependence of SBS.* Generalize the discussion of Section 9.3 to allow the angle θ between the laser and Stokes propagation directions to be arbitrary. In particular, determine how the Brillouin frequency Ω_B, the steady-state line-center gain factor g_0, and the phonon lifetime τ_p depend on the angle θ.
   [Ans.:

$$\Omega_B(\theta) = \Omega_B(\theta = 180^\circ) \sin\left(\tfrac{1}{2}\theta\right)$$
$$g_0(\theta) = g_0(\theta = 180^\circ) / \sin\left(\tfrac{1}{2}\theta\right)$$
$$\tau_p(\theta) = \tau_p(\theta = 180^\circ) / \sin^2\left(\tfrac{1}{2}\theta\right).]$$

3. *Transverse SBS.* Consider the possibility of exciting SBS in the transverse direction by a laser beam passing through a fused-silica window at near-normal incidence. Assume conditions appropriate to a high-energy laser. In particular, assume that the window is 70 cm in diameter and is uniformly filled with a laser pulse of 10-nsec duration at a wavelength of 350 nm. What is the minimum value of the laser pulse energy for which SBS can be excited? (In fact, transverse SBS has been observed under such conditions similar to those assumed in this problem; see, for example, J.R. Murray, J.R. Smith, R.B. Ehrlich, D.T. Kyrazis, C.E. Thompson, T.L. Weiland, and R.B. Wilcox, *J. Opt. Soc. Am.* 6, 2402 (1989).) [Ans.: ~2 kJ.]
4. *Optical damage considerations and the study of SBS.* The threshold intensity for optical damage to fused silica is approximately 3 GW/cm^2 and is of the same order of magnitude for most optical materials. (See, for example, W.H. Lowdermilk and D. Milam, *IEEE J. Quantum Electron.* 17, 1888 (1981).) Use this fact and the value of the SBS gain factor at line center quoted in Table 9.3.1 to determine the minimum length of a cell utilizing fused-silica windows that can be used to excite SBS in acetone with a collimated laser beam. Assume that the laser intensity is restricted to 50% of the threshold intensity as a safety factor to avoid damage to the windows. If the laser pulse length is 20 nsec, what is the minimum value of the laser pulse energy per unit area that can be used to excite SBS? (SBS is often excited by tightly focused laser beams rather than by collimated beams to prevent optical damage to the windows of the cell.)
5. *Pulse compression by SBS.* Explain qualitatively why the Stokes radiation excited by SBS in the backward direction can be considerable shorter in duration than the exciting radiation. How must the physical length of the interaction region be related to the duration of the laser pulse in order to observe this effect? Write down the coupled-amplitude equations

that are needed to describe this effect, and, if you wish, solve these equations numerically by computer. What determines the minimum value of the duration of the output pulse?
[Hint: Pulse compression by SBS is described in the scientific literature by D.T. Hon, *Opt. Lett.* 5, 516 (1980) and by S.S. Gulidov, A.A. Mak, and S.B. Papernyi, *JETP Lett.* 47, 394 (1988).]

6. *Brillouin-enhanced four-wave mixing*. In addition to SBS, light beams can interact in a Brillouin medium by means of the process known as Brillouin-enhanced four-wave mixing (BEFWM), which is illustrated in the figure shown below.

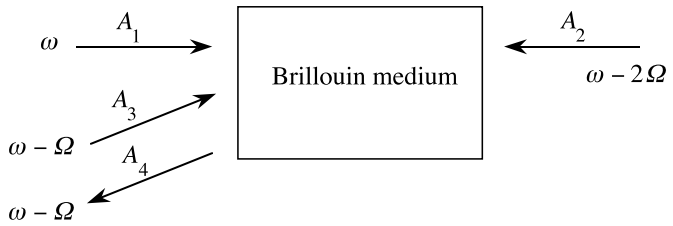

In this process, the incoming signal wave A_3 interferes with the backward-going pump wave A_2 to generate an acoustic wave propagating in the forward direction. The forward-going pump wave scatters from the acoustic wave to generate the phase-conjugate wave A_4. Since A_4 is at the Stokes sideband of A_1, it also undergoes amplification by the usual SBS process. Phase-conjugate reflectivities much larger than 100% have been observed in the BEFWM process. Using the general formalism outlined in Section 9.3, derive the form of the four coupled-amplitude equations that describe BEFWM under steady-state conditions. Solve these equations analytically in the constant-pump approximation.
[Hint: BEFWM has been discussed in the scientific literature. See, for example, M.D. Skeldon, P. Narum, and R.W. Boyd, *Opt. Lett.* 12, 1211 (1987).]

References

Suggested Further Reading on Stimulated Light Scattering

Boyd, R.W., Grynberg, G., 1992. Optical phase conjugation. In: Agrawal, G.P., Boyd, R.W. (Eds.), Contemporary Nonlinear Optics. Academic Press, Boston.

Fabelinskii, I.L., 1968. Molecular Scattering of Light. Plenum Press, New York.

Fabelinskii, I.L., 1975. Stimulated Mandelstam–Brillouin process. In: Rabin, H., Tang, C.L. (Eds.), Quantum Electronics: A Treatise, vol. I, part A. Academic Press, New York.

Fisher, R.A. (Ed.), 1983. Optical Phase Conjugation. Academic Press, New York; especially Chapters 6 and 7.

Kaiser, W., Maier, M., 1972. In: Arecchi, F.T., Schulz-DuBois, E.O. (Eds.), Laser Handbook. North-Holland.

Shen, Y.R., 1984. Principles of Nonlinear Optics. Wiley, New York.

Zel'dovich, B.Ya., Pilipetsky, N.F., Shkunov, V.V., 1985. Principles of Phase Conjugation. Springer-Verlag, Berlin.

Stimulated Brillouin Scattering

Bowers, M.W., Boyd, R.W., Hankla, A.K., 1997. Opt. Lett. 22, 360.
Boyd, R.W., Rzążewski, K., Narum, P., 1990. Phys. Rev. A 42, 5514.
Buckland, E.L., Boyd, R.W., 1996. Opt. Lett. 21, 1117.
Buckland, E.L., Boyd, R.W., 1997. Opt. Lett. 22, 676.
Carman, R.L., Shimizu, F., Wang, C.S., Bloembergen, N., 1970. Phys. Rev. A 2, 60.
Chiao, R.Y., 1965. Ph.D. dissertation. Massachusetts Institute of Technology.
Chiao, R.Y., Townes, C.H., Stoicheff, B.P., 1964. Phys. Rev. Lett. 12, 592.
Damzen, M.J., Hutchinson, H., 1983. IEEE J. Quantum Electron. QE-19, 7.
Gaeta, A.L., Boyd, R.W., 1991. Phys. Rev. A 44, 3205.
Gaeta, A.L., Skeldon, M.D., Boyd, R.W., Narum, P., 1989. J. Opt. Soc. Am. B 6, 1709.
Goldblatt, N., Hercher, M., 1968. Phys. Rev. Lett. 20, 310.
Goodman, J.W., 1985. Statistical Optics. Wiley, New York.
Gray, D.E. (Ed.), 1972. American Institute of Physics Handbook. McGraw-Hill, New York, pp. 3–37 ff.
Herman, R.M., Gray, M.A., 1967. Phys. Rev. Lett. 19, 824.
Hunt, F.V., 1955. J. Acoust. Soc. Am. 27, 1019; see also Gray (1972).
Kroll, N.M., 1965. Appl. Phys. 36, 34.
Kroll, N.M., Kelley, P.L., 1971. Phys. Rev. A 4, 763.
Kulagin, O., Pasmanik, G.A., Gaeta, A.L., Moore, T.R., Benecke, G.J., Boyd, R.W., 1991. J. Opt. Soc. B 8, 2155.
Loeb, L.B., 1961. The Kinetic Theory of Gases. Dover, New York.
Narum, P., Skeldon, M.D., Boyd, R.W., 1986. IEEE J. Quantum Electron. QE-22, 2161.
Narum, P., Skeldon, M.D., Gaeta, A.L., Boyd, R.W., 1988. J. Opt. Soc. Am. B 5, 623.
Pohl, D., Kaiser, W., 1970. Phys. Rev. B 1, 31.
Pohl, D., Maier, M., Kaiser, W., 1968. Phys. Rev. Lett. 20, 366.
Sette, D., 1961. In: Flügge, S. (Ed.), Handbuch der Physik, XI/1, Acoustics I. Springer-Verlag, Berlin.
Sidorovich, V.G., 1976. Sov. Phys. Tech. Phys. 21, 1270.
Zakharenkov, Y.A., et al., 2007. IEEE J. Sel. Top. Quantum Electron. 13, 473–479.
Zel'dovich, B.Ya., Popovichev, V.I., Ragulsky, V.V., Faizullov, F.S., 1972. JETP Lett. 15, 109.